

Dear Veronique Garçon,

together with this letter you receive the revised version of our manuscript submitted to Biogeosciences (ID: bg-2013-326).

Before going through your comments, I would like to thank you again on behalf of all authors for the thorough reading of our manuscript and constructive criticism which really helped improving the manuscript.

In the following I will go through your comments point by point including our feedback, is written in italic. After that point-by-point replies you find a list of the relevant changes.

Comment #1: In the Abstract, you say on Lines 9-11: to quantify the impact ...bottom: but it would be more instructive to the readers to actually say what are the processes playing the key role in controlling oxygen dynamics here. Alternatively, on Line 16: After Oxygen deficiency, a short sentence explaining why this higher susceptibility to O₂ deficiency in type (2) areas of the North Sea would be beneficial in the Abstract.

Reply: *We followed your alternative suggestion and included a clause which explains, why regions of type 2 are especially susceptible to O₂ deficiency (lines 16-19).*

Comment #2: We should find in the Abstract the answers to your 2 well formulated questions on lines 122-124 of the Introduction section.

Reply: *We extended the second last paragraph of the abstract to provide a brief overview which key parameters (of those used for the ODI) mainly control the O₂ dynamics in the southern, central and northern North Sea (22-28). We also adapted the last paragraph of abstract to explain why the southern central North Sea is especially susceptible to O₂ deficiency (lines 29-31).*

Comment #3: Section 2.2: Re-reading this sentence on lines 255-257: In addition.... grid cells occurs, I found it quite uneasy to understand the definition of MLD, can you rephrase?

Reply: *In the former Eq. (2) and the related description, we used both, the partial differential ($\partial T/\partial z$) and the corresponding difference quotient ($\Delta T/\Delta z$). While the first relates to the more physical point of view as it describes the vertical temperature gradient, the latter one relates to the representation of this gradient by the model and results from the discretisation of the model domain to the model grid. However, as it seems that this became not fully clear in the former version, we changed Eq. (2) in a way that it now directly uses the difference quotient ($\Delta T/\Delta z$), and changed the description of Eq. (2) correspondingly (lines 261-268). We hope this helped to clarify the definition of the MLD.*

Comment #4: Line 258: differ (without s)

Reply: *Thank you for finding this typo, we changed it according to your comment (line 269).*

Comment #5: You should move the definition of the Oxygen deficiency index (ODI) to section 2.4.2 in Section 2 Material and Methods. You argue in your response “that the problem is that the set of parameters, by which the ODI is described, and the equations actually are a result of the analysis based on Table 1 and the matching of simulated bottom O₂.” It is puzzling since the definition of a robust index should not depend on downstream results.

Reply: *We moved the definition of the ODI to Sect. 2.4.2 and adapted the description correspondingly (lines 365-411).*

Comment #6: Section 2.5: I would be cautious when you refer to interannual variability throughout the text, comparing 2 years (such as 2002 and 2010 line 372) does not constitute per se a proper interannual variability analysis, but simply a comparison of 2 years.

Reply: *We now do not use the term “inter-annual” anymore when referring to the comparison of*

only two years, which is the case in Sects. 2.5, 3.3.2, 3.4 (partly; incl. 3.4.1 and 3.4.2), 3.5 and 3.7. Instead we now either use “year-to-year variability” (n case of more than two years) or “variations between the two years”.

Comment #7: Section 3.1.1.: You can still reduce the length of the descriptive part on the evolution of bottom O₂ at North Dogger in 2007-2008 and at MARNET stations Ems in 2010-2011 (lines 399 to 438).

Reply: We applied some text reduction here reducing the line count from 40 to 34 (lines 447-480).

Comment #8: Line 437: besides these short-term changes in the difference ... are less than.

Reply: The “is less than” actually refers to “the difference”, hence it has to read as “is less than”. We put a comma right after “changes” to separate these two parts of the sentence more clearly (lines 479-480).

Comment #9: Section 3.1.3 Taylor diagrams for quantitative assessment of model performance are nowadays quite classical so I think you can omit having a subsection just on this. Rather insert at the end of section 3.1.1 the few lines on your figure 5 (time series) and end of section 3.1.2 the few lines on your figure 5 (spatially resolved data).

Reply: We followed this suggestion and moved the relevant parts to Sects. 3.1.1. (lines 491-500) and 3.1.2 (lines 560-570).

Comment #10: Line 616: Division of this mass...

Reply: Thank you for seeing this, we removed “the”.

Comment #11: On lines 615-617 you derive an estimate of the amount of time required for the consumption of the entire amount of O₂ available in V_{sub}. A few lines above (lines 612-614), you compute the daily O₂ consumption rate using a 6 months duration period. This is not clear to me.

Reply: Here, we assumed the average daily O₂ consumption rates calculated for the 6-months-period to be constant for each of the regions. Based on this we calculated the time needed to consume the total amount of O₂ available. This assumption, of course, is not realistic (as continuous consumption periods of several years are not in the case of the North Sea), however, we use it just to illustrate the large influence of organic matter export in combination with the magnitude of the sub-thermocline volume. To make this clearer we added a clause to this sentence (line 648).

Comment #12: Lines 687-688: Again I would not say the interannual variability here, but simply difference between years.

Reply: We changed this to “The variations of the minimum concentrations between the two years ...” (lines 673-674).

Comment #13: On Figures 8, 9 and 10 please enlarge all lines since some are hardly visible (yellow, green, light blue, light beige)

Reply: We increased the line width of all lines by factor 1.5, hoping that this improved the visibility sufficiently. We additionally increased the font size of the axes/colour scale labels in Figs. 4, 6-10.

Comment #13: I think section 3.4 can be shortened significantly by not detailing all the numerical values of all physical and biological processes for both years 2002 and 2010.

Reply: Where applicable, we removed numerical values for one of the two years in Sect. 3.4 (incl. 3.4.1 and 3.4.2) and also applied some further shortings. This reduced the line count from 103 to 91 (lines 711-801). Further reductions were not applied as we found it necessary to provide both values in some cases.

Comment #14: Line 815-816 : do you mean : however it is also visible...?

Reply: *Yes, this is exactly what we meant, thank you for this.*

Comment #15: Presently the conclusions section is far too long, there you should offer the reader a brief synthesis of the major findings of your study. Do not recall on which section (line 972) this was found for instance.

Reply: *We removed the reference to another section and also removed other less important information. By this we achieved a reduction in line count from 140 to 98 lines for the entire Conclusions section (lines 939-1036).*

Comment #16: Lines 982-984 should go as explanation in the abstract.

Reply: *We did as you suggested and added this to the abstract (lines 16-19; see also reply to comment #1).*

Comment #17: Section from lines 1043 until line 1104 can be shortened without losing much information.

Reply: *We worked on this part of the Conclusions and achieved a reduction in line count from 61 to 39 (lines 998-1036).*

List of relevant changes

1. Updated Figs. 4, 6-10 for better readability (thicker lines, increased font size of axes labels)
2. Updated abstract
3. Updated Eq. (3) and related description for easier understanding
4. Deleted Sect. 3.1.3 (now part of Sects. 3.1.1. and 3.1.2)
5. Moved definition of ODI (Eqs. (3)-(5) and description) from Sect. 3.3.2 to Sect. 2.4.2
6. Shortening of Sect. 4 (Conclusions and Perspectives)

With this we would like to conclude and thank you again for your support.

Kind regards

Fabian Große
on behalf of all authors

Attachments:

marked-up PDF file indicating all changes between the manuscript submitted after major revision and the newly revised version

Looking beyond stratification: a model-based analysis of the biological drivers of oxygen deficiency in the North Sea

**F. Große¹, N. Greenwood^{2,3}, M. Kreuz^{4,5}, H. J. Lenhart¹, D. Machoczek⁶, J. Pätsch⁵,
L. A. Salt⁷, and H. Thomas⁸**

¹University of Hamburg, Department of Informatics, Scientific Computing, Bundesstraße 45a,
20146 Hamburg, Germany

²Centre for Environment, Fisheries and Aquaculture Science (Cefas), Lowestoft, Suffolk, NR33
0HT, UK

³University of East Anglia, School of Environmental Sciences, Norwich, NR4 7TJ, UK

⁴University of Hamburg, Institute for Hydrobiology and Fisheries Science, Olbersweg 24, 22767
Hamburg, Germany

⁵University of Hamburg, CEN, Institute of Oceanography, Bundesstraße 53, 20146 Hamburg,
Germany

⁶Federal Maritime and Hydrographic Agency, Bernhard-Nocht-Straße 78, 20359 Hamburg,
Germany

⁷CNRS, UMR 7144, Equipe Chimie Marine, Station Biologique de Roscoff, Place Georges Teissier,
29680, Roscoff, France

⁸Dalhousie University, Department of Oceanography, 1355 Oxford Street, Halifax, Canada

Correspondence to: F. Große (fabian.grosse@uni-hamburg.de)

Abstract

Low oxygen conditions, often referred to as oxygen deficiency, occur regularly in the North Sea, a temperate European shelf sea. Stratification represents a major process regulating the seasonal dynamics of bottom oxygen, yet, lowest oxygen conditions in the North Sea do not occur in the regions of strongest stratification. This suggests that stratification is an important prerequisite for oxygen deficiency, but that the complex interaction between hydrodynamics and the biological processes drives its evolution.

In this study we use the ecosystem model HAMMOM-ECOHAM to provide a general characterisation of the different zones of the North Sea with respect to oxygen, and to quantify the impact of the different physical and biological factors driving the oxygen dynamics inside the entire sub-thermocline volume and directly above the bottom.

With respect to oxygen dynamics, the North Sea can be subdivided into three different zones: (1) a highly productive, non-stratified coastal zone, (2) a productive, seasonally stratified zone with a small sub-thermocline volume, and (3) a productive, seasonally stratified zone with a large sub-thermocline volume. Type 2 reveals the highest susceptibility to oxygen deficiency due to sufficiently long stratification periods (> 60 days) accompanied by high surface productivity resulting in high biological consumption, and a small sub-thermocline volume implying both a small initial oxygen inventory and a strong influence of the biological consumption on the oxygen concentration.

Inter-annual Year-to-year variations in the oxygen conditions are caused by variations in primary production, while spatial differences can be attributed to differences in stratification and water depth. ~~In addition, we~~ The large sub-thermocline volume dominates the oxygen dynamics in the northern central and northern North Sea and makes this region insusceptible to oxygen deficiency. In the southern North Sea the strong tidal mixing inhibits the development of seasonal stratification which protects this area from the evolution of low oxygen conditions. In contrast, the southern central North Sea is highly susceptible to low oxygen conditions (type 2).

We furthermore show that benthic bacteria diagenetic processes represent the main oxygen consumers in the bottom layer, consistently accounting for more than 50 % of the overall consumption. Thus, primary production followed by remineralisation of organic matter under stratified conditions constitutes the main driver for the evolution of oxygen deficiency in the southern central North Sea. By providing these valuable insights, we show that ecosystem models can be a useful tool for the interpretation of observations and the estimation of the impact of anthropogenic drivers on the North Sea oxygen conditions.

1 Introduction

Low oxygen (O_2) conditions (concentrations $< 6 \text{ mg } O_2 \text{ L}^{-1}$; OSPAR-Commission, 2003), often referred to as O_2 deficiency, occur regularly in the North Sea. A major process regulating the seasonal dynamics of bottom O_2 is the occurrence and duration of thermal stratification (e.g., Greenwood et al., 2010; O'Boyle and Nolan, 2010), which limits the vertical exchange of O_2 between the oxygenated surface layer and the deeper layers. In combination with events of enhanced primary production, and the subsequent degradation of organic matter, this favours the evolution of O_2 deficiency (e.g., Diaz and Rosenberg, 2008). Although the northern North Sea reveals strongest stratification, lowest O_2 concentrations occur in the central North Sea, which is shallower and where the duration of stratification is shorter and shows highest inter-annual year-to-year variability. Thus, one can argue that stratification is an important prerequisite for O_2 deficiency, but its severity and duration is controlled by the complex interaction between the hydrodynamical condition and the biogeochemical processes involved.

The North Sea is a temperate, semi-enclosed shelf sea adjacent to the northeastern Atlantic ocean. It has an average depth of about 90 m (Ducrottoy et al., 2000) with northward increasing bottom depth. The North Sea circulation is characterised by a cyclonic pattern mainly driven by the southward Atlantic inflow across the shelf edge defining its northern boundary. Lenhart and Pohlmann (1997) showed that about 85 % of the incoming Atlantic water is recirculated north of the Dogger Bank, a shallow area with water depth less than

55 40 m and 300 km of zonal extent at about 55° N, 2° E (Kröncke and Knust, 1995). The circulation south of the Dogger Bank is governed by the inflow through the English Channel and follows the continental coast. At the southern tip of Norway it joins the Norwegian coastal current leaving the North Sea at its northern boundary.

60 Stratification in the North Sea reveals some substantial regional differences. While the shallower southern parts are permanently well-mixed due to the strong influence of the M_2 tidal component (Otto et al., 1990), the deeper parts north of 54° N reveal seasonal, mostly thermal stratification (e.g., Burt et al., 2014; Pingree et al., 1978; van Leeuwen et al., 2015). Seasonal haline stratification occurs to a lesser extent along the Norwegian coast. The transition between these permanently mixed and seasonally stratified regions occurs gradually (Pingree et al., 1978). In consequence, even areas relatively near to the coast, which are affected by high riverine nutrient run-off, often reveal stratified conditions at sub-seasonal timescales (e.g., Burt et al., 2014).

70 In the 1980s, events of O_2 deficiency reaching values below $3 \text{ mg } O_2 \text{ L}^{-1}$ occurred regularly in the stratified southeastern central North Sea and in the German Bight (Brockmann and Eberlein, 1986; Brockmann et al., 1990; Rachor and Albrecht, 1983). During [this](#) [that](#) time, the problem of low O_2 conditions in the North Sea reached public awareness in relation to eutrophication as demersal animals died across a large area due to these low O_2 concentrations (von Westernhagen et al., 1986). Eutrophication, or in other words, high anthropogenic nutrient loads mainly supplied by rivers (Brockmann et al., 1988; Jickells, 1998; Rabalais et al., 2010), may raise the ambient nutrient concentrations followed by an increase in biomass production. Under given physical conditions, eutrophication thus causes an enhanced supply of organic matter sinking into the subsurface layer and reinforces O_2 consumption near the sea floor due to bacterial remineralisation.

80 Even though the second International Conference on the Protection of the North Sea (INSC-2) prescribed a 50 %-reduction of river nutrient loads (inorganic nitrogen and phosphorus) in order to mitigate the effects of eutrophication (de Jong, 2006), Fig. 1 shows that O_2 deficiency remains a persistent problem in the North Sea up to the present day. According to Kemp et al. (2009) these events can be classified as “persistent seasonal”. Low

85 bottom O₂ concentrations may cause death of benthic organisms or fish eggs as well as
avoidance of the affected areas by benthic species. Therefore, low O₂ concentrations consti-
tute a major indicator of eutrophication (category 3 indicator, i.e., “evidence of undesir-
90 able disturbance”; OSPAR-Commission, 2003) and concentrations lower than 6 mg O₂ L⁻¹
result in the classification as “problem area” in terms of eutrophication within the OSPAR
assessment (Claussen et al., 2009). In the present study the term “oxygen deficiency” is
used in this OSPAR context rather than “hypoxia”. While O₂ deficiency is clearly defined
within OSPAR by the 6 mg O₂ L⁻¹ threshold, hypoxia refers to the negative impact of low O₂
concentrations on organisms. An overview of the impact of hypoxia on marine biodiversity
can be found in Vaquer-Sunyer and Duarte (2008). Further descriptions on the ecological
disturbance of different levels of low O₂ concentrations are summarised by Friedrich et al.
95 (2014) and Topcu et al. (2009).

Despite the relevance of the bottom O₂ concentrations for the assessment of the ecologi-
cal status of an ecosystem, O₂ measurements are sparse and either temporally or spatially
limited. In addition, it is difficult to place the measurement at the right time and location to
obtain a comprehensive picture of the duration and spatial extent of summer O₂ deficiency
100 (Friedrich et al., 2014). One way to address this problem is to analyse the representative-
ness of available data with respect to eutrophication assessment (Brockmann and Topcu,
2014).

Only in recent years continuous measurements for the North Sea have become available
by, ~~for instance~~ e.g., the SmartBuoy programme of Cefas (Centre for Environment, Fisheries
and Aquaculture Science, UK; Greenwood et al., 2010) or the MARNET programme (MA-
Rine Monitoring NETwork in the North Sea and Baltic Sea) of the BSH (Federal Maritime
and Hydrographic Agency, Germany). These monitoring programmes provide daily time se-
ries of O₂ and related parameters (e.g., temperature, salinity, chlorophyll) in different depths
and allow for the analysis of the temporal evolution of stratification and O₂ concentrations
110 at the location of observation.

Greenwood et al. (2010) published the first data from continuous measurements of bot-
tom O₂ concentrations for two sites (“North Dogger” and “Oyster Grounds”) in a European

shelf sea. Using these measurements, the dynamic interaction between stratification and the evolution towards low bottom O_2 concentrations can be observed, as well as the rapid
115 recovery to saturated O_2 conditions after the breakdown of stratification due to mixing in autumn. However, even these continuous measurements did not provide sufficient information to fully understand the processes which caused the observed O_2 evolution. Greenwood et al. (2010) and Queste et al. (2013), who extended the locally confined findings by Greenwood et al. (2010) to the spatial scale using survey data from August 2010 and ICES
120 historical data, refer to “plausible mechanisms” like vertical mixing or advection when the measurements could not be explained in detail. In consequence, Greenwood et al. (2010) stated, that the data provided insight into the processes affecting the O_2 dynamics but models are required to further elucidate the significance of the seasonal drivers.

Ecosystem models produce ~~temporally and spatial~~ temporally and spatially consistent
125 picture on O_2 and can therefore provide insight into the balance between the physical and biological factors and processes governing the evolution of the bottom O_2 concentrations. Thus, they can help ~~to~~ understand and interpret measurements of O_2 and related parameters and can further describe the history of events of low O_2 conditions.

In this study we use the three-dimensional physical-biogeochemical model system
130 HAMSOM-ECOHAM to provide a detailed description of the current state of the North Sea in terms of its O_2 conditions, and the processes leading to low bottom O_2 concentrations. The interpretation of the model results will enable the following questions to be answered: What are the main drivers for the O_2 dynamics in the various subregions of the North Sea? Why are certain North Sea regions more susceptible to low O_2 conditions than others despite similar stratification patterns?
135

For this purpose, we first validate the simulated bottom O_2 concentrations with respect to their temporal evolution and spatial distribution in order to show that the model captures the main features. Subsequently, we present a regional characterisation of the parameters controlling the bottom O_2 dynamics and propose a simple O_2 deficiency index which extends
140 this characterisation to the entire North Sea. Finally, we ~~analyse~~ attribute the individual contributions of the governing processes ~~in terms of inter-annual and regional variability in~~

~~their individual contribution to the~~ to the temporal and spatial variability of the overall O_2 evolution, ~~including a detailed interpretation~~ under particular consideration of the continuous O_2 measurements at North Dogger (Greenwood et al., 2010).

2 Material and methods

2.1 The ECOHAM model

Our study is based on the coupled physical-biogeochemical model system HAMSOM-ECOHAM. The physical model HAMSOM (HAMBurg Shelf Ocean Model; Backhaus, 1985) is a baroclinic primitive equation model using the hydrostatic and Boussinesq approximation (Pohlmann, 1991). HAMSOM provides the temperature (T) and salinity (S) distribution, in addition to the advective flow fields and the vertical turbulent mixing coefficient, which are used as forcing for the biogeochemical model ECOHAM (ECOsystem model HAMBurg). For a detailed description of HAMSOM the reader is referred to Pohlmann (1991). Further information on the application of HAMSOM can be found in Backhaus and Hainbucher (1987) and Pohlmann (1996).

The biogeochemical model ECOHAM (Lorkowski et al., 2012; Pätsch and Kühn, 2008) represents the pelagic and benthic cycles of carbon (C), nitrogen (N), phosphorus (P), silicon (Si) and O_2 . The O_2 module within the ECOHAM model incorporates physical and biogeochemical processes determining the pelagic O_2 concentrations (Pätsch and Kühn, 2008).

The air-sea exchange of O_2 at the sea surface constitutes an important physical **factor process** besides the effects of advective transport and vertical diffusion in the interior water column. The air-sea flux of O_2 in the present application is parametrised according to Wanninkhof (1992). In relation to the biology, the O_2 cycle is linked to the C cycle by photosynthesis, zooplankton respiration and bacterial remineralisation. While photosynthesis is a source of O_2 , the latter ones act as O_2 sinks. A further sink of O_2 is nitrification, the bacterial transformation of ammonium to nitrate. Within ECOHAM, this process is light-

dependent and links the O_2 cycle to the N cycle. Nitrification only occurs under aerobic conditions (i.e., concentrations $> 0 \text{ mg } O_2 \text{ L}^{-1}$), which is a realistic constrain for the pelagic
170 North Sea environment. It is light-dependent, being stronger under low light conditions. Pelagic denitrification is implemented, but is negligible as it only occurs under anaerobic conditions. Pelagic anaerobic ammonium oxidation (anammox) is not implemented, however, it can be neglected for the same reason. Except for primary production, the biological processes involved in the O_2 cycle are not temperature-dependent in the present model
175 setup.

For the representation of the benthic remineralisation processes a simple sediment module is used. A layer of zero extent is defined below the deepest pelagic layer of each water column. There the deposited organic matter is collected and remineralised (Pätsch and Kühn, 2008). The benthic remineralisation of the organic matter is defined as a first-order
180 process with relatively high remineralisation ~~rates~~ (C, N, P) and dissolution rates (Si; opal) preventing year-to-year accumulation of deposited matter. The released dissolved inorganic matter is returned directly into the pelagic bottom layer. Different ~~remineralisation~~ rates are applied to organic C, N, P and Si (~~opal~~), resulting in different time scales for the release into the pelagic. In ECOHAM, the O_2 cycle is affected by the benthic remineralisation in a direct
185 and indirect way. First, the remineralisation in the sediment is accompanied by the direct reduction of the O_2 concentrations in the pelagic bottom layer above. Second, inorganic nitrogen is released from the sediment in the form of ammonium, which can be nitrified within the water column under O_2 consumption. According to Seitzinger and Giblin (1996), who suggested a tight coupling between benthic nitrification and denitrification, benthic denitrification depends on the benthic O_2 consumption in our model. Direct benthic nitrification
190 and benthic anammox are neglected as the sediment has zero vertical extent (Pätsch and Kühn, 2008).

For a more detailed description of the ECOHAM model, including the full set of the differential equations and parameter settings of ECOHAM, the reader is referred to Lorkowski et al. (2012). A detailed description and analysis of the O_2 module can be found in Müller
195 (2008).

2.1.1 Model setup and forcing data

The model domain extends from ~~+5.25~~15.250° W to 14.083° E and from 47.583 to 63.983° N and comprises the entire North Sea, large parts of the northwestern European continental shelf and parts of the adjacent northeastern Atlantic. The horizontal resolution is $1/5^\circ$ with 82 grid points in latitudinal direction and $1/3^\circ$ with 88 grid points in longitudinal direction. The horizontal grid of the model domain is shown in Fig. 2. The vertical dimension with a maximum depth of 4000 m is resolved by 31 z-layers with a surface layer of 10 m. The vertical has a resolution of 5 m between 10 and 50 m depth, which is relevant for the calculation of the MLD (Sect. 2.2). Below 50 m, the layer thicknesses successively increase with depth.

The model system was run over the period 1977 to 2012. HAMSOM was initialised with a monthly-averaged climatology based on the World Ocean Atlas (WOA; Conkright et al., 2002). The meteorological forcing was derived from NCEP/NCAR reanalysis data (Kalnay et al., 1996; Kistler et al., 2001) and provides 6 hourly information for air temperature, cloud coverage, relative humidity, wind speed and direction. Short wave radiation was calculated from astronomic insolation and cloud coverage applying a correction factor of 0.9 (Lorkowski et al., 2012). The data were interpolated to the model grid and time step according to O'Driscoll et al. (2013) and Chen et al. (2014). Daily freshwater run-off data for 249 rivers were provided by Cefas and represent an updated dataset of that used by Lenhart et al. (2010) covering the entire simulation period. The same dataset encompassed nutrient loads used for the ECOHAM.

At open boundaries, surface elevation was prescribed as a fixed (Dirichlet) open boundary condition (OBC) according to the M2 tide, while for horizontal transport velocities radiation OBCs were applied. For tracers (T and S) radiation and radiative-nudging OBCs were used in the case of inflow and outflow, respectively. A detailed description of the OBCs is provided by Chen et al. (2013). The HAMSOM simulation was carried out with a 10 min time step.

225 ECOHAM was run off-line with a time step of 30 min using the 24-hour averages of the hydrographic and hydrodynamic fields generated by HAMSOM. In the model setup used, short wave radiation is attributed to the first layer (surface) only and the specific effect of light attenuation due to SPM and planktonic self-shading on the thermal structure is not taken into account. A sensitivity study allowing for deeper light penetration and feedback on the thermal structure confirmed this effect to be only of minor importance (not shown).

230 For the biogeochemical state variables a climatology of depth-dependent monthly averages was prescribed at the boundaries and solely for DIC yearly changing data were provided (Lorkowski et al., 2012). To include the effect of SPM on the light climate, a daily climatology from Heath et al. (2002) was used. Data for atmospheric N deposition were compiled using a hybrid approach. This was required since the overall simulation period
235 (1977–2012) exceeds the period of data available from the EMEP (Cooperative program for monitoring and evaluation of the long-range transmissions of air pollutants in Europe) model (1995–2012). First, the EMEP results for total deposition of oxidised (NO_x) and reduced nitrogen (NH_3) were interpolated to the model grid. Second, we calculated the average annual deposition rates for the NO_x and NH_3 for each grid cell, based on the 1995–2012
240 EMEP data. The resulting spatially resolved arrays of average deposition rates were subsequently normalised by the spatial average of the entire domain to yield the spatially resolved anomaly fields. Finally, gridded deposition rates for individual years were obtained using (1) the gridded anomaly fields, (2) EMEP’s spatially averaged (over our model domain) deposition rates for year 2005, and (3) long-term trends (normalised towards year 2005) for the temporal evolution of European emissions of NO_x and NH_3 (Fig. 2 in Schöpp et al., 2003).
245 The output of the biogeochemical simulation was stored as daily values (cumulative fluxes, state variable snapshots) for the entire domain and simulation period.

2.2 Extracting stratification parameters from model results

250 Stratification constitutes the prerequisite for the potential evolution of low O_2 conditions in the North Sea. In this study (1) its duration and (2) the mixed layer depth (MLD) are used to describe stratification. Seasonal stratification in the North Sea is mainly T -driven (Burt

et al., 2014), except for the regions of haline stratification along the Norwegian coast. As observations do not cover the entire model domain and simulation period we determined the duration of stratification and the MLD from the simulation results. For this purpose we developed a simple 2-step algorithm based on T . First, the stratified period is determined using a temperature difference criterion:

$$S_{\text{strat}}(x, y, t) = \begin{cases} 1 & \Delta T|_{-H}^0(x, y, t) \geq 0.05 \text{ K} \\ 0 & \text{otherwise} \end{cases} \quad (1)$$

S_{strat} is a switch defining if a water column at location (x, y) and time t is stratified ($S_{\text{strat}} = 1$) or not ($S_{\text{strat}} = 0$) depending on the temperature difference ΔT between the surface and bottom depth H . The critical temperature difference $\Delta T_{\text{crit}} = 0.05 \text{ K}$ was determined by evaluating different ΔT_{crit} against the temporal evolution of simulated bottom O_2 at different locations within the model domain. In addition, periods of stratified conditions are only considered as such, if they last for at least 5 days without any interruption. Otherwise bottom waters are considered to be ventilated again.

In the second step, in the case of stratification the MLD is defined as the depth D where the vertical temperature gradient $\delta T / \delta z$ has its maximum: of a model water column is determined using the vertical T gradient $\Delta T / \Delta z$:

$$\text{MLD}(x, y, t) = \begin{cases} D(\max(\delta \Delta T / \delta \Delta z)) & S_{\text{strat}}(x, y, t) = 1 \\ 0 & \text{otherwise} \end{cases} \quad (2)$$

In addition, the discrete model grid implies the definition of the MLD as the bottom depth of the upper of the two layers between which the maximum gradient $\Delta T / \Delta z$ is calculated for each grid cell interface within the considered water column. ΔT represents the T difference between two vertically adjacent model layers and Δz represents the distance between the centre points of two vertically adjoining grid cells occur these two grid cells. D is then defined as the depth level of the interface where $\Delta T / \Delta z$ has its maximum. As the described stratification and MLD criterion differs differ significantly from common MLD criteria (e.g., Table 1 in Kara et al., 2000), an evaluation is provided in Appendix A.

2.3 Validation data

280 For the validation of the model results we used observation data from different sources. The datasets can be subdivided into two types: (1) temporally resolved, localised data and (2) spatially resolved “snapshots”. The first type was used for the validation of the seasonal evolution of O₂, whereas the second type was used to validate the general spatial patterns and **inter-annual** year-to-year variability of bottom O₂ during late summer.

285 2.3.1 Localised, temporally resolved data – Cefas-SmartBuoy and MARNET

Cefas operates a network of SmartBuoys to provide autonomous in situ measurements of physical, chemical and biological parameters (Mills et al., 2005). A SmartBuoy was located directly north of the Dogger Bank (‘North Dogger’) at 55°41′ N, 2°16.80′ E (see Fig. 2, region 2) between 24 February 2007 to 15 September 2008 in 85 m water depth (Greenwood et al., 2010). O₂ concentrations were continuously recorded with a frequency of 5 Hz at 31 m and 85 m . These autonomous O₂ measurements were corrected for drift using O₂ concentrations determined from discrete water samples to give an accuracy of 0.5 % (Greenwood et al., 2010). For validation purposes the O₂ data derived from the sensor at 85 m depth were used.

295 The BSH operates a continuous monitoring station at 54°10′ N, 6°21′ E (see Fig. 2, region 1; hereafter referred to as station “Ems”). The O₂ saturation is measured hourly using opto-chemical sensors (optodes). Sensors are located in 6 and 30 m depth, respectively, and the bottom depth is 33 m. The applied sensors have a resolution of 0.03 mg O₂ L⁻¹ and an accuracy better than 0.26 mg O₂ L⁻¹. Before deploying the sensors a 0–100 % calibration is conducted, and they are re-calibrated after operation to quantify any drift. In addition, 300 a regular on-site validation takes place using a calibrated fast optode (accuracy of ± 2 %) or by applying the Winkler titration (accuracy better than ± 1 %).

2.3.2 Spatially resolved “snapshot” data – the North Sea programme

During the North Sea programme, carried out by the Royal Netherlands Institute for Sea
305 Research (NIOZ) with support from the Dutch Science Foundation (NWO) and the Euro-
pean Union, the North Sea was sampled from 18 August to 13 September 2001, and from
17 August to 5 September 2005 and 2008. The North Sea was covered by an approximate
 $1^\circ \times 1^\circ$ grid, sampling approximately 90 stations in each of the years (Bozec et al., 2005,
2006; Salt et al., 2013). During each cruise, a total of 750 water samples were collected
310 for dissolved O_2 . In 2001, the O_2 concentrations were determined by the Winkler titration
using a potentiometric end-point determination with an accuracy of $\pm 2 \mu\text{mol } O_2 \text{ kg}^{-1}$ (less
than $\pm 0.07 \text{ mg } O_2 \text{ L}^{-1}$ depending on T and S). In 2005 and 2008, the O_2 concentrations
were obtained applying the spectrophotometric Winkler approach with a precision of less
315 than $0.03 \text{ mg } O_2 \text{ L}^{-1}$. A detailed description of the measurement system used is given in
Reinthaler et al. (2006).

The data available were gridded to the model grid (Fig. 2). In the case of multiple mea-
surements for the same model grid cell and date, the average of these measurements was
used for validation. To compare our model results to these data, we calculated the averages
and standard deviations of our simulation over the observation period of the corresponding
320 year.

2.4 Deriving a regional O_2 characterisation of the North Sea

2.4.1 Identification of the key parameters

For the development of a regional O_2 characteristic, potential controlling factors were anal-
ysed in relation to bottom O_2 . Besides stratification, eutrophication is considered as a major
325 driver for developing low O_2 conditions (e.g., Diaz and Rosenberg, 2008; Kemp et al., 2009).
Thus, primary production within the mixed layer and the resulting organic matter export into
the layers below the MLD must be considered to be the main source for degradable organic

matter. In addition, organic matter can be advected from surrounding waters in the form of phyto- or zooplankton and detritus, subsequently sinking out of the mixed layer.

330 Another important criterion is the water volume below the thermocline (Druon et al., 2004). A smaller volume separated from the surface due to stratification holds a lower initial inventory of O_2 than a larger volume even though concentrations ~~are~~ can be similar or even higher in the smaller volume. Thus, our set of O_2 -related characteristics consists of: mixed layer primary production (PP_{mld}), horizontal advection of organic matter into and out of the
335 mixed layer ($ADH_{\text{org,in}}$ and $ADH_{\text{org,out}}$; including phyto-/zooplankton and detritus), vertical organic matter export below the MLD (EXP_{org} ; only detritus) and mixing of O_2 below the MLD (MIX_{O_2}), and the sub-MLD volume V_{sub} .

To detect regional characteristics within the North Sea area, we defined four different sub-domains encompassing 4×4 model water columns each (see Fig. 2, red boxes): (A) southern North Sea (SNS) under strong tidal influence, (B) southern central North Sea (SCNS) with high ~~inter-annual~~ year-to-year variability in stratification, (C) northern central North Sea (NCNS) with a dominant summer stratification each year, and (D) northern North Sea (NNS) with a dominant summer stratification each year and a strong influence of the Atlantic. For all these regions, the parameters described above were calculated for the years
340 2000–2012 relative to a reference depth D_{ref} , which is defined as the bottom depth of the model layer directly below the annual maximum MLD among all four regions. We decided to use a $D_{\text{ref}} > \text{MLD}$ to ensure that for the different regions all parameters were determined on a comparable level. This implies that the values for PP_{mld} , $ADH_{\text{org,in}}$ and $ADH_{\text{org,out}}$ are integrated from the surface to D_{ref} , whereas EXP_{org} and MIX_{O_2} are the vertical fluxes through
345 D_{ref} . The same D_{ref} was applied to all regions, but ~~inter-annual~~ year-to-year variations were allowed.

To determine the annual maximum MLD, we first calculated the stratification period for the 4×4 -regions B–D using Eq. (1). Region A was excluded from this calculation as no persistent MLD developed due to tidal mixing. In this context, $S_{\text{strat}}(t)$ of a region is only 1 if
350 $S_{\text{strat}}(x, y, t) = 1$ for all 16 water columns within a 4×4 -region. The daily MLD for each water column within a region was calculated by applying $S_{\text{strat}}(t)$ to Eq. (2), and subsequently the

daily MLD of the region is defined as the median of these 16 daily values. The annual MLD for each region was then determined as the median of this daily time series. Finally, the annual maximum MLD among all 4 regions is used to determine the reference depth D_{ref} , which is defined as the bottom depth of the layer directly below this maximum MLD.

The values for these O_2 -related quantities were calculated for individual years relative to D_{ref} and temporally integrated over the period from 1 April to 30 September (hereafter ‘summer’). Consequently, the average values over the entire period 2000–2012 are calculated and presented in Table 1, additionally including the average O_2 concentrations at the beginning and end of the summer period as well as the average duration of stratification.

2.4.2 Development of a spatially resolved index for North Sea O_2 deficiency

In order to obtain a North Sea wide indicator for O_2 deficiency under stratified conditions, it is necessary to extend the regionally confined characteristic described in the previous section. For this purpose, we extract the key factors affecting O_2 from this regional information and combine them into a single index – the oxygen deficiency index (ODI). The ODI aims to represent the main spatial and temporal patterns of O_2 deficiency in the North Sea under stratified conditions, while being as simple as possible and incorporating only a very limited number of parameters.

~~For the calculation of the ODI, we first calculate individual indices for the different parameters taken into account. These~~ Stratification period, organic matter export and sub-thermocline volume are considered as the key parameters controlling the bottom O_2 dynamics. Surface primary production can be used as a proxy for organic matter export assuming that most of the exported organic matter is produced locally. Bottom depth can be used as an indicator for the sub-MLD volume assuming only minor fluctuations of the MLD during the summer stratified period. In addition, the bottom depth directly influences the amount of organic matter reaching the bottom layer relative to the amount being produced near the surface, due to the exposure of sinking matter to pelagic remineralisation. Thus, the following key factors are used for the calculation of this index: (longest continuous)

stratification period (t_{strat} ; in days), summer surface primary production (PP_{mld} ; in g C m^{-2} ; 1 April to 30 September), and bottom depth (D_{bot} ; in m).

First, individual dimensionless indices are calculated for each of these quantities. The individual indices range between 0 and 1, indicating conditions counteracting and supporting O_2 deficiency, respectively. ~~These indices are calculated for each grid point within the model domain. Consequently, these spatially resolved individual indices are combined into the ODI also yielding values between 0~~ The calculation of the stratification and production indices, I_{strat} and I_{pp} , is based on the work by Druon et al. (2004) and reads as:

$$I_{Q_i}(x, y) = \min \left(1, \max \left(0, \frac{Q_i(x, y) - Q_{i,\text{min}}}{Q_{i,\text{max}} - Q_{i,\text{min}}} \right) \right), \text{ with } Q_1 = t_{\text{strat}}, Q_2 = I_{\text{pp}}. \quad (3)$$

$I_{Q_i}(x, y)$ represents the index corresponding to the actual value of the quantity $Q_i(x, y)$ with its defined upper and lower thresholds, $Q_{i,\text{max}}$ and $Q_{i,\text{min}}$. For t_{strat} , $Q_{i,\text{max}}$ and $Q_{i,\text{min}}$ are set to 50 and 150 days, respectively. Stratification periods of less than 50 days are considered to be too short to facilitate the evolution of O_2 deficiency, respectively deficiency, while periods longer than 150 days are considered as seasonally well-stratified. The lower threshold for PP_{mld} was set to 120 g C m^{-2} as PP_{mld} does not reach lower values in most parts of the North Sea. The upper threshold was set to 200 g C m^{-2} as such high values and even higher are simulated in the southeastern North Sea.

For the depth index, I_{D} , a different definition was chosen as lowest O_2 concentrations occur in areas of intermediate depth, where seasonal stratification can develop and the O_2 inventory is limited due to a small volume below the thermocline. Therefore, we defined I_{D} as follows:

$$I_{\text{D}}(x, y) = \begin{cases} \max \left(0, \frac{D_{\text{bot}}(x, y) - D_{\text{min}}}{D_{\text{peak}} - D_{\text{min}}} \right) & D_{\text{bot}}(x, y) < D_{\text{peak}} \\ 1 - \min \left(1, \frac{D_{\text{bot}}(x, y) - D_{\text{peak}}}{D_{\text{max}} - D_{\text{peak}}} \right) & \text{otherwise.} \end{cases} \quad (4)$$

D_{bot} represents the actual bottom depth at location (x, y) . $D_{\text{peak}} = 40$ m is the bottom depth we found to be most favourable for O_2 deficiency in the North Sea. The lower threshold $D_{\text{min}} = 25$ m corresponds to the maximum MLD we found for the shallower southern North Sea. The upper threshold $D_{\text{max}} = 90$ m was chosen to exclude the areas where the initial O_2 inventory is sufficient to prevent O_2 deficiency due to the large volume below the thermocline.

Finally, the ODI combines the three individual indices according to the following equation:

$$\text{ODI}(x, y) = I_{\text{D}}(x, y) \cdot \sum_{i=1}^2 w_{Q_i} I_{Q_i}(x, y), \text{ with } w_{Q_1} = 1/4, w_{Q_2} = 3/4. \quad (5)$$

Here, I_{Q_i} and w_{Q_i} represent the index for a quantity and the related weight, respectively. The values for t_{strat} are referred to by Q_1 and those for PP_{mld} by Q_2 . The equation for ODI implies that it is zero in areas where $I_{\text{D}} = 0$. The stronger weighting of PP_{mld} implies that variations in the ODI between different years are more strongly affected by variations in summer surface productivity than by the duration of stratification.

The ODI ranges between 0 (low risk of O_2 deficiency) and 1 (high risk) and is calculated for each water column (x, y) within the model domain. By this we obtain a spatially resolved indicator for O_2 deficiency is found which helps to in the North Sea, which helps regionalise the North Sea in terms of O_2 conditions.

The definition of the ODI, which was found to provide a good qualitative representation of the bottom conditions is presented in Sect. 3.3.2, together with the resulting spatial distribution for the years 2002 and 2010.

2.5 Quantification of driving processes: spatial and temporal variability, and data interpretation

In order to quantify the processes driving the O_2 dynamics in different regions, and to analyse their inter-annual variability, we calculated O_2 mass balances for three different

regions encompassing 2×2 grid cells (see Fig. 2, regions 3–5). First, mass balances for the entire volume below the thermocline (hereafter “sub-MLD”) in region 3 are compared with the corresponding bottom layer mass balances to identify differences between the bottom layer dynamics and the dynamics within the entire sub-MLD volume. This is done for two years, 2002 and 2010, to analyse ~~inter-annual variations~~ variations between these years. Region 3 was chosen as it shows the lowest bottom O_2 concentrations within the entire model domain, with the overall minimum in 2002 and relatively high concentrations in 2010. The daily resolved MLD defines the upper integration limit for the sub-MLD mass balances, i.e., the integration depth may vary during the stratified period. The daily MLD is defined as the vertical level of the model grid which is closest to the daily average MLD of the 2×2 -region according to Eqs. (1) and (2).

Second, we compare the O_2 mass balances of the bottom layer for the regions 4 and 5 in 2002 with that of region 3 to unveil regional differences. In a last step the mass balance analysis is applied to interpret the O_2 evolution observed at North Dogger (see Fig. 2, region 2).

The O_2 concentrations and saturation concentrations shown in the different mass balances represent the average values within the analysed volume. Values of O_2 saturation concentrations were calculated according to Benson and Krause (1984) using simulated T and S . The fluxes presented are cumulative changes in the O_2 concentrations of the considered volume, i.e., the values at the end of the stratified period reflect the total net change of the O_2 concentrations due to the corresponding physical or biological process. Positive and negative values at the end of the stratification period indicate net gain and loss, respectively. The slope of each line represents the intensity of the corresponding flux at the specific moment in time, i.e., a steep positive (negative) slope implies a strong gain (loss) effect.

3 Results and discussion

3.1 Model validation

3.1.1 Temporal evolution of bottom O₂

460 Figure 3 shows the comparison of simulated bottom O₂ against time series data at the Cefas station North Dogger for the years 2007 (a) and 2008 (b) and the MARNET station Ems during 2010 (c) and 2011 (d). The indicated stratification period was derived from the simulated temperature fields using Eq. (1).

At North Dogger, observed and simulated bottom O₂ concentrations show a steady decrease ~~beginning with~~ after the onset of stratification. While stratification according to Eq. (1) starts a bit earlier compared to that described by Greenwood et al. (2010), the beginning of the decrease in bottom O₂ concentrations coincides well. The simulated and observed O₂ concentrations at this time are in good agreement.

Some small-scale fluctuations in the observations ~~like the minimum in the concentrations at 15 April 2007;~~ are not fully reproduced by the simulation. ~~However,~~ however, the general evolution is represented well by the model. The average O₂ reduction in the simulation is slightly less than in the observations, visible in the difference between the concentrations at beginning and end of the stratified period. ~~The decrease in the concentrations in 2007 suddenly ends with a mixing event between 10 and 12 November.~~ Stratification ends a bit earlier in the simulation, with the result that simulated bottom O₂ starts to recover while the observed concentrations continue to decline, ~~reaching a minimum of 6.4~~. The observed O₂ concentration at the end of the stratified period is about 6.8 mg O₂ L⁻¹, while the simulation results in about 7.4 mg O₂ L⁻¹.

In 2008, we can see a similar slight overestimation of simulated O₂ concentrations, but less than in ~~2007 which is again due to a faster decline in the observations. As in 2007;~~ ~~some minor fluctuations visible~~ 2007. Some minor fluctuations in the observations are again not represented by the model, but the general trend evolution of bottom O₂ is represented well ~~by the simulation~~. It should be noted, that ~~at station North Dogger, the centre depth of~~

the model bottom layer is equal to the different depths of the time series (76 (bottom depth of 485 82m); while the sampling was conducted in for simulation, 85 m depth. This for observation) may also affect the difference between simulated and observed O₂ concentrations.

At MARNET station Ems the observed bottom O₂ concentrations show significantly larger 490 intra-seasonal fluctuations than at North Dogger. This applies to both years 2010 and 2011, and mainly results from the shallower station depth, i.e., sampling depth (sensor in 30 m). ~~The water column of the model at this location encompasses 6 vertical layers and is 35 deep with a centre depth of the deepest grid cell of~~ As at North Dogger, differences may also relate to different depths of the time series (32.5 m for observation) and the vertical resolution with only 6 layers.

In 2010, the onset of O₂ decline in the observations is in good agreement with the 495 ~~beginning of the decline in the simulated concentrations~~ that in the simulations. Stratification lasts shorter and is less persistent than at North Dogger. ~~From late May to late June, the observed bottom reveals a steep decrease which is not fully represented in the simulation; but shows the remarkable drop in observed in the second half of June and the subsequent increase in bottom~~ As at North Dogger, intra-seasonal fluctuations in the O₂ , even though 500 ~~to a lesser extent. However, it has to be noted that the evolution are not fully reproduced.~~ The model tends to overestimate bottom O₂ in 2010, revealing a maximum difference of about 1 mg O₂ L⁻¹.

In 2011, persistent stratified periods derived from the simulation do not exceed 2 months at station Ems. Consequently, the temporal evolution of bottom O₂ represents mainly the 505 temporal evolution of the O₂ saturation concentrations. Again large fluctuations of up to ± 2 mg O₂ L⁻¹ can be seen in the observations which are not fully reproduced by the model. Besides these short-term changes, the difference between simulated and observed bottom concentrations is less than 0.8 mg O₂ L⁻¹ with higher summer values in the simulation.

The validation of bottom O₂ at the stations North Dogger and Ems shows that the 510 HAMSOM-ECOHAM model is capable of reproducing the main features of the bottom O₂ dynamics at these two stations. The minor differences in the concentrations (< ± 0.4 mg O₂ L⁻¹) at the beginning and end of the year, representing mainly the saturation

concentrations, show that the general physical setting provided by the model is reasonable. The slightly slower O₂ reduction in the simulation may indicate an underestimation of the biological consumption, e.g., due to benthic remineralisation. Intra-seasonal fluctuations at both stations are not fully reproduced, due to the limited spatial resolution of the model grid. Additionally, the tides may have an effect at station Ems on the short-term. However, they are not resolved due to the daily time step of the simulated current fields.

The generally good agreement between simulation and observation is also shown by the Taylor diagram (Taylor, 2001, see Fig. 5, markers “a” for North Dogger and “b” for Ems), which presents the correlation coefficients (COR), STDs and centred root-mean-square differences (RMSD) of the simulation relative to the observations. STDs and RMSDs are normalised by the STD of the corresponding observations. For analysis, the data of each dataset was merged into a continuous series of data. For both stations, COR is high with values of about 0.95 and the normalised RMSD is less than 0.38. The RMSD values are mainly due to the larger range and higher (seasonal and intra-seasonal) variability in the observed bottom O₂, which is also indicated by the normalised STDs of about 0.73 and 0.82 for Cefas North Dogger and MARNET Ems, respectively.

3.1.2 Spatial distribution of late summer bottom O₂

Figure 4 shows the spatial distribution of the average simulated and observed O₂ concentrations in the model bottom layer for the years 2001 (a), 2005 (b) and 2008 (c), and the standard deviation (STD) related to the averages in 2005 (d). The averaging period for the simulations corresponds to the complete observation period for each year, listed in the bottom right corner of each panel.

In 2001, the observations show the lowest concentrations of all years with minimum values of 5.9 mg O₂ L⁻¹ in the area 54–57° N, 4.5–7° E. This minimum is similarly present in the model yielding 6.96 mg O₂ L⁻¹. Maximum observed concentrations were found off the southern tip of Norway (9.3 mg O₂ L⁻¹) and in the deepest parts of the Norwegian Trench (8.7 to 8.8 mg O₂ L⁻¹). The very high observed value at the northwesternmost sampling site represents an outlier due to the decreasing vertical resolution of the model in greater depth.

In 2005, the observed minimum values are about $0.3 \text{ mg O}_2 \text{ L}^{-1}$ higher than in 2001. This relative increase compared to 2001 is reproduced well by the simulation showing a similar increase by about $0.2 \text{ mg O}_2 \text{ L}^{-1}$. The observations show lowest bottom O_2 a bit north and south of the simulated minimum, but still relatively low values less than $7.2 \text{ mg O}_2 \text{ L}^{-1}$ in the centre of the simulated minimum. Highest observed concentrations of $9.3 \text{ mg O}_2 \text{ L}^{-1}$ are located in the very deep area at the eastern end of the Norwegian Trench, and in the inner German Bight. In the German Bight, the model indicates only slightly higher values as compared to 2001, while in the northern North Sea, the simulation shows lower values as compared to 2001, which can be seen in the observations as well.

In 2008, the observations reveal significantly higher bottom O_2 concentrations in the area of the 2001 minimum, compared to the previous years. In contrast, observed concentrations in most other parts of the North Sea are lower than in 2001 and 2005. The overall minimum concentration in 2008 of $7.2 \text{ mg O}_2 \text{ L}^{-1}$ is reached close to the Dutch coast. In the southern North Sea, the simulation yields lower bottom O_2 concentrations, and significantly higher values in the 2001 minimum area. For the western central and northern North Sea the picture is different. Here, the observations result in consistently lower values as compared to 2001 and 2005, whereas the simulated O_2 shows higher values in most areas, except for the eastern Norwegian Trench.

The simulated STD in 2005 is mainly representative for the years 2001 and 2008 as well. It shows that in most areas of the North Sea the changes in bottom O_2 during August/September are very low throughout a period of 3 to 4 weeks, indicated by a STD of less than $0.1 \text{ mg O}_2 \text{ L}^{-1}$. The observations also show only small STDs in most areas.

In general, the basin-wide distributions of simulated bottom O_2 represent the observed spatial patterns and their inter-annual-year-to-year variations quite well, even though absolute values are not always reflected. Both observed and simulated bottom O_2 concentrations show that the 50 m-isobath (broadly along 54° N , 0° E to 57° N , 8° E ; Thomas et al., 2005) marks the separation line between the northern regions unaffected by low O_2 conditions and the southeastern parts, which are more vulnerable to low O_2 concentrations. In addition, the model demonstrated it is capable of capturing inter-annual variations in the

570 bottom O_2 evolution [between different years](#). In combination with the results of the time series validation (Sect. 3.1.1), this confirms that the described model setup provides reliable information on the internal physical and biological processes driving the O_2 dynamics in the North Sea.

575 The small STD of simulated bottom O_2 confirms that using the averages over a period of up to 4 weeks provides a reasonable measure for most areas. In addition, these small values imply that measurements taken late August/early September (before the breakdown of stratification) can be considered as a representative synoptic picture of the late summer bottom O_2 conditions. However, the [validation presented in Sect. 3.1.1 time series validation](#) showed that in some areas lowest concentrations of bottom O_2 may occur remarkably later in the year (see Fig. 3a). Consequently, the picture obtained from observations taken in August/September does not necessarily reflect the spatial distribution of minimum bottom O_2 concentrations, which underlines the importance of choosing the appropriate point in time for the monitoring of low O_2 conditions.

585 The small STD of the observations, which is a result of the data gridding, shows that in most regions vertical O_2 gradients near the bottom are negligible. The high values of 0.75 and 0.59 $mg O_2 L^{-1}$ southeast of the Dogger Bank and northwest of Denmark, respectively, result from the fact that values above and below the thermocline were taken into account for the averaging.

3.1.3 A quantitative assessment of the model performance

590 ~~The Taylor diagram (Fig. 5; Taylor, 2001) provides a quantitative assessment of the model performance with respect to simulated bottom concentrations in relation to the validation data used in Sect. 3.1.1 and Sect. 3.1.2. For this purpose, we merged the observations and corresponding simulation data of the different years into one continuous series of data for each of the three datasets. The Taylor diagram presents the correlation coefficients (COR), STDs and centred root-mean-square differences (RMSD) of the simulation relative to the observations. STDs and RMSDs are normalised by the STD of the corresponding observations.~~

The statistics As for the time series data confirm the good agreement between simulation and observation shown in Fig. 3. For both stations, COR is high with values of about 0.95 and the normalised RMSD is less than 0.38. The RMSD values are mainly due to the larger range and higher (seasonal and sub-seasonal) variability in the observed bottom, which is also indicated by the normalised STDs of about 0.73 and 0.82 for Gefas North Dogger and MARNET Ems, respectively. For 5 (marker c) shows the statistical measures of the validation for the spatially resolved data. Here, COR reaches only about 0.64. This lower correlation was also shown which is also indicated in Fig. 4 by the inter-annual variations in the simulations and observations variations between year 2008 and the previous years, when the simulation revealed a relative change inverse to that in the observations in the northern North Sea. The normalised RMSD of 0.77 is about twice as high as for the time series, which can be attributed to the greater regional differences in the observed bottom O_2 concentrations with higher maximum and lower minimum values. The normalised STD equals 0.67 which also indicates the less strong spatial gradients in the simulation. These statistics confirm the picture given by Fig. 4, which showed that the spatial patterns in the observed bottom O_2 concentrations are basically reproduced by the model, with only slight shortcomings with respect to the amplitude of the bottom O_2 concentrations and inter-annual year-to-year variations in some regions of the North Sea.

In summary, the validation based on time series and spatially resolved observations showed that our model system is capable of reproducing the main temporal (seasonal and inter-annual) and spatial features of bottom in the North Sea. Hence, the analysis of the dynamics based on HAMSOM-ECOHAM will provide valuable insight in temporal and spatial variations of the North Sea dynamics.

3.2 Simulated stratification periods and minimum bottom O_2

Figure 6a and b show the spatial distribution of the longest persistent stratification periods (after Eq. (1) using simulated T) for the years 2002 and 2010, respectively. Both years show similar stratification patterns with stratification periods of > 180 days in large parts of the central and northern North Sea.

630 Comparing the corresponding minimum concentrations of bottom O_2 (Fig. 6c and d) ~~the simulation results show~~shows significant differences. The minimum bottom O_2 concentrations in 2002 in the region from $55\text{--}56.5^\circ$ N, $4.5\text{--}7.5^\circ$ E constitute the lowest O_2 concentrations during the entire period 2000–2012 reaching values of below $5.8\text{ mg } O_2\text{ L}^{-1}$. In contrast, the duration of stratification in this area is similar or even longer in 2010 than in 2002. The O_2 concentrations in 2002 are even below the O_2 threshold applied by OSPAR ($6\text{ mg } O_2\text{ L}^{-1}$; OSPAR-Commission, 2005) and persist for about one month (not presented). In contrast, 2010 represents a year with relatively high minimum bottom O_2 concentrations being above $7.3\text{ mg } O_2\text{ L}^{-1}$ in the entire model domain. The areas directly north and south
635 of the Doggerbank also reveal lower bottom O_2 concentrations in both years.

The stratification periods derived from the simulation are in good agreement with the different stratification regimes described by Pingree et al. (1978) and van Leeuwen et al. (2015). The latter applied a density-based stratification criterion on model results to subdivide the North Sea into areas of different stratification characteristics, and showed that
640 most areas of the seasonally stratified central and northern North Sea reveal stratification periods of 170 to 230 days.

The increased potential for low O_2 conditions north and south of the Doggerbank corresponds well to observed bottom O_2 time series in these regions (Greenwood et al., 2010). Queste et al. (2013) also observed lower bottom O_2 concentrations north of the Dogger
645 Bank in August 2010, however, they found the minimum concentrations a bit further north around 57° N.

The discrepancy between minimum O_2 concentrations in the two years and the quite similar stratification patterns demonstrates that stratification is an important prerequisite for low O_2 conditions, but other physical or biological factors do have a strong effect on the O_2
650 dynamics in the North Sea.

3.3 An O₂-related characteristic of the North Sea

3.3.1 Key parameters

Table 1 shows the 2000–2012 summer (1 April to 30 September) averages of the quantities considered as potentially relevant for O₂ for the regions A–D (see Fig. 2). The quantities were calculated relative to a D_{ref} of 25 m. In addition, the stratification period (t_{strat}), average MLD (D_{mld}), average bottom depth (D_{bot}) and area of the regions are provided.

The mixed layer net primary production, PP_{mld} , is strongest in the coastal region A and shows decreasing values towards the central North Sea. In the SCNS region B, PP_{mld} accounts for about 87 % of that in the highly productive coastal region A. The corresponding value for the NCNS region C and NNS region D is about 80 % and 88 %, respectively.

Despite the highest PP_{mld} in the coastal region A, the SCNS region B shows the strongest contribution of gross advection of organic matter, $ADH_{\text{org,in}}$ and $ADH_{\text{org,out}}$. Both regions show positive net advection of organic matter, while the two northern regions C and D are characterised by negative net advection, i.e., advective loss in organic matter. The latter regions are located north of the Dogger Bank, thus, they are affected by the northern Atlantic inflow. In this region, net advection results in a loss in organic matter as the recirculated northward flowing water has higher concentrations of organic matter than the incoming Atlantic water.

The vertical export of organic matter, EXP_{org} , below D_{ref} consistently adds up to about 12–14 % of PP_{mld} , indicating the clear link between these quantities. Region B yields an EXP_{org} of 75 % of that in the coastal region A, which corresponds ~~with~~ to a higher net advective import of organic matter of 6.7 g C m⁻² in region A, compared to only 1.6 g C m⁻² in Region B. EXP_{org} in region C and D reach about 69 % and 79 % relative to region A, respectively.

The vertical mixing of O₂, MIX_{O_2} , is highest within the coastal region A and adds up to 116.1 g O₂ m⁻², which is due to strong tidal mixing. The stratification period, t_{strat} , of 151 days in region B is shorter than in region C (220 days) and does not cover the entire summer period. Thus, MIX_{O_2} in region B is significantly larger than in regions C and D.

680 The evolution of the O_2 concentrations between the beginning and end of the summer period reveals some interesting aspects in relation to the previously mentioned parameters. The O_2 concentrations at 1 April show significant differences between the regions ranging between $9.5 \text{ mg } O_2 \text{ L}^{-1}$ (region C and D) and $10.1 \text{ mg } O_2 \text{ L}^{-1}$ (region A). The O_2 concentrations at the 30 September yield values between $7.7 \text{ mg } O_2 \text{ L}^{-1}$ (region A) and $8.3 \text{ mg } O_2 \text{ L}^{-1}$ (region D). This implies a consistently decreasing O_2 consumption during summer from region A to D. This spatial gradient in the O_2 consumption is opposite to that in t_{strat} , which shows a steady increase from region A to D.

685 In order to give an impression of the impact of EXP_{org} on the O_2 dynamics of the water volume below the MLD, V_{sub} , we link the amount of exported organic matter to the amount of O_2 available within V_{sub} assuming the organic matter is remineralised completely in the area of settlement. Based on the O_2 concentration at the beginning of April, the total amount of O_2 available is 1365 kt for region B and 4590 kt for region C. The total amount of exported organic matter is calculated as the product of EXP_{org} and the total area of the considered region. This calculation yields 130 kt C and 115 kt C for the regions B and C, respectively. As O_2 consumption and C release occur with a molar ratio of 1 : 1 during bacterial remineralisation (Neumann, 2000), we obtain the daily O_2 consumption by dividing by the total duration of the considered ~~6s-period~~ 6-months-period (=183 days), yielding 0.71 and $0.63 \text{ kt } O_2 \text{ d}^{-1}$ for region B and C, respectively.

695 The initial O_2 mass is calculated as the product of the initial O_2 concentration and V_{sub} . ~~Division of the~~ Assuming the daily O_2 consumption to be constant for each region, division of this mass by the daily consumption rate calculated above provides an estimate of the amount of time required for the consumption of the entire amount of O_2 available in V_{sub} . This calculation yields a period of about 2 years for region B, whereas the corresponding value for region C is significantly higher with almost 12 years. This great difference between the resulting periods (factor 6), compared to the relatively small difference between the daily consumption rates (factor 1.1), illustrates clearly the large influence of the sub-MLD volume, V_{sub} , on the temporal evolution of the O_2 concentrations below the MLD.

The same calculation based on the threshold of $6 \text{ mg O}_2 \text{ L}^{-1}$ used by OSPAR (OSPAR-Commission, 2005) yields a consumption period of 283 days for region B, which indicates the relatively high potential for O_2 deficiency in this region.

710 This characteristic based on the four different North Sea regions demonstrated that the duration of stratification alone cannot explain the temporal evolution of sub-MLD O_2 concentrations. It shows the great importance of the organic matter export which drives the biological O_2 consumption. In addition, the volume below the MLD plays a key role as it governs the amount of O_2 which is available throughout the stratified period, and in combination with the organic matter export defines whether O_2 deficiency may occur or not. 715 Thus, these three quantities can be considered as the key parameters for governing the O_2 dynamics of the seasonally stratified North Sea.

3.3.2 The oxygen deficiency index (ODI)

720 ~~With the definition of the ODI, we aim for a simple approach to represent the main spatial and temporal patterns of deficiency in the North Sea. Therefore, in the first step a further simplification of the key parameters found in the previous section is worthwhile. The strong link between organic matter export and surface primary production allows for the use of the latter one as a proxy. Bottom depth can be used as an indicator for the sub-MLD volume assuming only minor fluctuations of the MLD during the summer stratified period. In addition, the bottom depth directly influences the amount of organic matter reaching the bottom layer, relative to the amount being produced near the surface.~~

730 ~~Finally, the following key factors are used for the calculation of this index: (longest continuous) stratification period (t_{strat} ; in), summer surface primary production (PP_{MLD} ; in ; 1 April to 30 September), and bottom depth (D_{bot} ; in). The individual dimensionless indices for these three quantities, ranging between 0 and 1, are calculated differently. The calculation of the stratification and production indices, I_{strat} and I_{pp} , is based on the work~~

by Druon et al. (2004) and reads as:-

$$I_{Q_i}(x, y) = \min \left(1, \max \left(0, \frac{Q_i(x, y) - Q_{i,\min}}{Q_{i,\max} - Q_{i,\min}} \right) \right), \text{ with } Q_1 = t_{\text{strat}}, Q_2 = I_{\text{pp}}.$$

$I_{Q_i}(x, y)$ represents the index corresponding to the actual value of the quantity $Q_i(x, y)$ with its defined upper and lower threshold, $Q_{i,\max}$ and $Q_{i,\min}$. For t_{strat} the upper and lower threshold are set to 50 and 150 days, respectively. These values were found by comparing the spatial distributions of simulated t_{strat} and minimum bottom for the entire period 2000–2012. Minimum stratification periods in regions with relatively low minimum bottom concentrations are about 60 days, and areas with stratification periods of above 150 days are considered as seasonally well-stratified. The lower threshold for PP_{mid} was set to 120as PP_{mid} does not reach lower values in most parts of the North Sea. The upper threshold was set to 200as such high values and even above are simulated in the southeastern North Sea.

For the depth index, I_D , a different definition was chosen as the highest potential for deficiency occurs in areas of intermediate depths, where seasonal stratification can develop and the inventory is limited due to a small volume below the thermocline. Therefore, we defined I_D as follows:-

$$I_D(x, y) = \begin{cases} \frac{\max \left(0, \frac{D_{\text{bot}}(x, y) - D_{\text{min}}}{D_{\text{peak}} - D_{\text{min}}} \right)}{1} & D_{\text{bot}}(x, y) < D_{\text{peak}} \\ \frac{1 - \min \left(1, \frac{D_{\text{bot}}(x, y) - D_{\text{peak}}}{D_{\text{max}} - D_{\text{peak}}} \right)}{1} & \text{otherwise.} \end{cases}$$

D_{bot} represents the actual bottom depth at location (x, y) . $D_{\text{peak}} = 40\text{m}$ is the bottom depth we found to be most favourable for deficiency in the North Sea. The lower threshold $D_{\text{min}} = 25\text{m}$ corresponds to the maximum MLD we found for the shallower southern North Sea. The upper threshold $D_{\text{max}} = 90\text{m}$ was chosen to exclude the areas where the initial inventory is sufficient to prevent deficiency due to the large volume below the thermocline.

Finally, the ODI combines the three individual indices according to the following equation:

$$\text{ODI}(x, y) = I_D(x, y) \cdot \sum_{i=1}^2 w_{Q_i} I_{Q_i}(x, y), \text{ with } w_{Q_1} = 1/3, w_{Q_2} = 2/3.$$

Here, I_{Q_i} and w_{Q_i} represent the index for a quantity and the related weight, respectively. The values for t_{strat} are referred to by Q_1 and those for PP_{mid} by Q_2 . The equation for ODI implies that it is zero in areas where $I_D = 0$. The stronger weighting of PP_{mid} implies that inter-annual variabilities in the ODI are more strongly affected by variations in summer surface productivity than by the duration of stratification.

The ODI ranges between 0 (low risk of deficiency) and 1 (high risk). It is calculated for each water column (x, y) within the model domain to obtain a spatially resolved picture of the risk of deficiency in the North Sea.

The ODI resulting from the simulated stratification duration (t_{strat}), summer surface primary production (PP_{mid}) and model topography for the years 2002 and 2010 is shown in Fig. 7a and b, respectively. It can be seen that the ODI tends to be higher in 2002 than in 2010 in the region where minimum bottom O_2 is lowest in both years (see Fig. 6). The North of the Doggerbank, the ODI also shows slightly higher values in the region directly north of the Doggerbank which corresponds with than in the surrounding waters which corresponds to the lowered bottom O_2 in this region. The inter-annual variability variations of the minimum concentrations between the two years in this region is are also well-reproduced by the ODI. Especially in 2002, the highest ODI coincides with the lowest concentrations in the entire domain. In 2010, the highest ODI is located a bit south of the minimum O_2 concentrations, which is mainly caused by the high surface production in this region. Along the northern British coast, the ODI also shows high values for both years which is in good agreement with the slightly lower minimum bottom O_2 in this area, however. However, ODI values tend to be too high and do not represent the slightly lower minimum O_2 concentrations off the eastern Scottish coast around 57–58°N as the bottom depth in this area exceeds 90 m (i.e., $I_D = 0$). Directly northwest of Denmark, the ODI also yields higher high

values for both years with higher values in 2002. This corresponds well ~~with to~~ the simulated bottom O_2 concentrations in this area, even though ODI values are too high, compared to ODI values in the central North Sea.

785 With respect to the factors selected for the calculation of the ODI, Table 1 shows that stratification alone is not sufficient to explain the North Sea O_2 dynamics. While the reduction in the O_2 concentrations is steadily decreasing from region A to D, stratification duration is characterised by a steady increase from region A (80 days) to D (226 days). Regarding the PP_{mld} , the strongest O_2 reduction occurs in the regions of highest productivity A and B. In the northern regions, the higher PP_{mld} in region D does not correspond ~~with to~~ stronger
790 reduction in O_2 . As t_{strat} is also higher in this region, ~~another a further~~ factor is needed to describe the basic O_2 dynamics. The reduced effect of surface production in the northernmost area is likely to result from the dilution effect due to the higher V_{sub} . Considering the bottom depth D_{bot} as a proxy for V_{sub} , it is shown that the strongest decrease occurs in the shallower regions A and B with average depths of about 40 m, while the regions deeper
795 than 90 m (C and D) show a weaker decrease.

Net advection of organic matter, which is not taken into account in the ODI, appears to be of minor importance for subsurface O_2 relative to the local surface production as the net advective input of organic matter is significantly less than the local production. The O_2 concentrations at the beginning of the stratified period were also not taken into account as they show lower values in regions with higher minimum concentrations and vice versa.
800

In summary, the ODI represents well the spatial and ~~inter-annual temporal~~ variations of minimum bottom O_2 concentrations despite the small set of controlling factors. This confirms that a simple combination of only stratification duration, organic matter production and bottom depth is sufficient to reproduce the main spatial and temporal patterns of the minimum bottom O_2 in the seasonally stratified North Sea. Thus, the findings from Table 1
805 can be applied to most parts of the North Sea. In addition, the similarity of the ODI inside the regions analysed in Sect. 3.3.1 and inside the regions selected for the mass balance analyses (see Fig. 2, regions 2–4) and their surrounding areas shows that these regions

810 can be considered as representative, allowing for a meaningful analysis of the O_2 dynamics in these regions.

3.4 Driving mechanisms and ~~inter-annual~~ year-to-year variability of sub-thermocline O_2 dynamics

815 The previous analyses showed that stratification constitutes a necessary condition for ~~low~~ O_2 ~~conditions, but inter-annual~~ deficiency, but year-to-year variations especially in the biological factors mainly control the O_2 dynamics. ~~However, for a~~ For a better understanding of the processes controlling sub-thermocline O_2 ~~-controlling processes below the thermocline, and the interplay of physics and biology,~~ a more detailed analysis is provided by the mass balances in Fig. 8. As the bottom O_2 dynamics are also influenced by the processes in the mid-water, Fig. 8a and b show the O_2 mass balances for the sub-MLD volume (V_{sub}) in region 3 (see Fig. 2) for the years 2002 and 2010, respectively.

820 The stratification characteristics are similar for both years, with an average MLD of ~~15.19~~ about 15 m and ~~15.99~~ a stratification period (grey area) of 187 for ~~2002 and 2010, respectively.~~ days in both years, only differing by a later onset (and breakdown) of stratification in 2010. The temporal evolution of the MLD (dash-dotted grey) is also similar, with deeper MLDs at the beginning and end of the stratified period and few events of enhanced mixing, ~~indicated by mixed layer deepening,~~ during the summer months (May to August). ~~The stratification period (grey area) lasts 187 in both years, only differing by a later onset (and breakdown) in 2010 (11 March) compared to 2002 (31 March).~~

830 The sub-MLD O_2 concentration (solid magenta) at the beginning of the stratified period in 2002 is about $9.81 \text{ mg } O_2 \text{ L}^{-1}$, being about $0.33 \text{ mg } O_2 \text{ L}^{-1}$ lower than in 2010. At the end of stratification, the 2002 value of $6.85 \text{ mg } O_2 \text{ L}^{-1}$ is about $0.81 \text{ mg } O_2 \text{ L}^{-1}$ lower than in 2010. ~~Accordingly, the net decrease in during the 2002 stratified period is by factor 1.2 higher than in 2010.~~

835 In 2002, the clearly diverging temporal evolution of simulated O_2 and the corresponding saturation concentrations ($O_{2,\text{sat}}$; dash-dotted magenta) reveals that the different O_2 evo-

lution is caused not only by decreasing O_2 solubility. Hence, other factors must play an important role for the O_2 evolution below the MLD.

3.4.1 The influence of advection and mixing

The comparison of advection (ADV_{O_2} ; including horizontal and vertical components; dashed light blue) and vertical mixing (MIX_{O_2} ; turbulent diffusion; dashed dark blue) for the years 2002 and 2010 shows strong ~~annual and inter-annual variations~~ variations between the two years. ADV_{O_2} regularly changes its influence on the sub-MLD O_2 concentrations during stratification in both years. However, ~~comparing~~ considering the temporally integrated effect, ADV_{O_2} causes a net gain of about $25.8 \text{ g } O_2 \text{ m}^{-2}$ in 2002, whereas in 2010 it results in a ~~net loss of about 7.0~~ slight net loss in O_2 . Advection positively affects the O_2 concentrations during the last 2–3 weeks of the stratified period in both years. ~~In 2002, this strong increase is accompanied by and even causes~~ a net increase in the concentrations. O_2 increase in 2002.

The vertical mixing of O_2 through the mixed layer (MIX_{O_2}) adds up to $26.9 \text{ g } O_2 \text{ m}^{-2}$ ~~and +8.3~~ in 2002 ~~and (1.5-fold of 2010, respectively value)~~. In late April and late June 2002, two events of enhanced mixing cause a rapid gross increase in the O_2 concentrations, in the latter case even resulting in a net increase in O_2 . During August 2002, MIX_{O_2} even has a negative effect on O_2 , which coincides with a very shallow MLD of 10 m (= bottom of first model layer). In 2010, this negative effect on O_2 is even more persistent, ~~lasting from late April to mid-August~~. The increased positive net effect of ADV_{O_2} and MIX_{O_2} ~~during the in 2002 stratified period~~ relates to the stronger spatial O_2 gradients due to the local O_2 minimum in region 3.

The daily rates of change in O_2 (averaged over the stratification period) due to these factors for the different years provide a comparable measure of their effect on sub-MLD O_2 , independent of the duration of stratification. The averages of these daily rates for the entire period 2000–2012 result in $0.008 \pm 0.060 \text{ g } O_2 \text{ m}^{-2} \text{ d}^{-1}$ for ADV_{O_2} and $0.153 \pm 0.042 \text{ g } O_2 \text{ m}^{-2} \text{ d}^{-1}$ for MIX_{O_2} . The small positive value average value and the large STD for ADV_{O_2} ~~shows show~~ that on average, ~~advection~~ is only a minor source of O_2 , how-

865 ever, ~~the large STD indicates the large inter-annual variability during the analysed period.~~ This implies that advection can provide both, a remarkable gain or loss, during different years with large year-to-year variability. The average and STD for MIX_{O₂} show that vertical mixing consistently causes a net increase in sub-MLD O₂.

3.4.2 Biological drivers of the sub-thermocline O₂ dynamics

870 In contrast to the integrated effect of the physical factors, Fig. 8a and b ~~shows~~ show that the biological processes cause a net loss in O₂. The only source process for O₂ is primary production (PP; dashed light blue) which causes a gross increase of about 61.8 g O₂ m⁻² and 44.5 in 2002 and (1.4-fold of 2010, respectively value). Considering the biological sink processes, pelagic remineralisation of organic matter (REM_{pel}; dashed light green) has the strongest effect on the sub-MLD O₂, accounting for 50 % of the overall biological consumption. 875 Benthic remineralisation (REM_{sed}; dashed yellow) accounts for 18.8 %, while zooplankton respiration (RES_{zoo}; dashed dark green) and nitrification (NIT; dashed red) contribute 22 % and 8.8 %, respectively. This order in the relative importance is a consistent picture consistent throughout the entire period 2000–2012 (not shown).

In 2002, REM_{pel} is strongest among all years ~~2000–2012 causing an consumption of about yielding~~ -103.1 g O₂ m⁻². ~~In contrast, while~~ 2010 represents the year with the lowest of weakest REM_{pel} being about 26.0 less than in 2002. For RES_{zoo} 2010 yields a value of 24.7, 2002 yields a value of -45.1 g O₂ m⁻² which represents only 55 of the 2002 value (1.8-fold of 2010 value). The 2002 and 2010 values constitute the highest and lowest among all years, respectively. The same applies to REM_{sed} with a 2002 value of 885 -28.5 g O₂ m⁻², and a (1.2-fold of 2010 value of -23.3 (61 of 2002 value)). NIT is also strongest in 2002 resulting in -18.1 g O₂ m⁻². ~~In 2010, NIT shows values, while in 2010 it is~~ about 13 % below the average value of -13.0 ± 2.5 g O₂ m⁻².

890 The integrated effect of all biological sink processes (REM_{pel}, REM_{sed}, RES_{zoo} and NIT) adds up to -204.8 g O₂ m⁻² in 2002, and to and to -136.4 g O₂ m⁻² in and 2010, i.e., the total biological O₂ consumption in 2002 is 1.5 times higher than in 2010 and 1.2 times higher than the 2000–2012 average of 169.9 ± 21.2 g O₂ m⁻². The relative contri-

895 bution of the individual processes to the ~~overall~~ biological O_2 consumption shows only minor ~~inter-annual~~ variations during the analysed period. REM_{pel} ~~has an average relative contribution of~~ contributes to $53.6 \pm 1.7\%$, while REM_{sed} accounts for $17.2 \pm 0.9\%$. For RES_{zoo} and NIT the average ~~relative~~ contributions result in $21.6 \pm 1.5\%$ and $7.6 \pm 0.8\%$, respectively. The ~~export of organic matter~~ EXP_{org} below 25 m depth (not presented; calculation analogous to Table 1) in 2002 is nearly 1.6 times larger than in 2010, which is in good agreement with the differences in the integrated effect of the biological O_2 sinks.

900 ~~Considering the interaction of physical and biological processes, two events of enhanced mixing in~~ In late April and late June 2002 (Fig. 8a) two events of enhanced mixing reveal direct and indirect effects ~~of enhanced vertical mixing~~ on the biological processes. The ~~mixing-induced~~ renewal of the nutrient pool causes short-term increases in PP around the MLD. ~~Consequently, the consumption due to which in turn enhances~~ RES_{zoo} and REM_{pel} ~~is enhanced. In addition, the increased~~ EXP_{org} ~~also enhances~~ REM_{pel} . ~~The change in the concentrations during these events shows that~~. Consequently, only the stronger event in late June causes a net increase in O_2 , ~~whereas continuously decreases during the weaker event in late April~~. It should be noted that the shown strengthening in the different biological effects is also influenced by the change in the MLD (i.e., integration depth), however, it is also visible when considering a constant MLD (not shown).

910 ~~Furthermore~~, PP shows the strongest effects on sub-MLD O_2 when the MLD is shallowest, ~~which indicates the existence of a deep chlorophyll maximum~~ in the layer between 10 and 15. This also (DCM). This explains the negative influence of MIX_{O_2} during these periods as O_2 concentrations are highest in this layer within the DCM due to high PP. The ~~generally~~ only minor positive or even negative effect of MIX_{O_2} during most ~~parts~~ of the stratified period ~~also~~ emphasises the importance of stratification for the sub-MLD O_2 dynamics as it efficiently limits the O_2 supply into these layers.

920 The good agreement between the ~~inter-annual differences~~ variations in EXP_{org} and the integrated effect of the biological O_2 sinks between the two years confirms that the supply of detrital matter to the deep layers is the driving force of sub-MLD O_2 consumption. The strong influence of pelagic remineralisation demonstrates its crucial role for the bottom O_2

concentrations as it directly affects the potential O_2 supply from the mid-water into the bottom layer.

3.5 Bottom layer dynamics of the North Sea O_2 minimum zone

Even though the dynamics in the mid-water affect the bottom O_2 levels, lowest concentrations occur in the bottom layer. In order to show which processes are the main contributors to the O_2 dynamics in this layer, Fig. 8c and d show the mass balances for the bottom layer in region 3 for 2002 and 2010. The average bottom depth in this region is 47.75 m, and the model bottom layer encompasses a volume of about 14.4 km³.

The O_2 concentrations at the beginning of the stratified period, 9.79 and 10.12 mg O_2 L⁻¹ for 2002 and 2010, respectively, are similar to those in V_{sub} . The concentrations at the end of stratification, 6.76 mg O_2 L⁻¹ in 2002 and 7.55 mg O_2 L⁻¹ in 2010, show larger differences to those for V_{sub} .

The effect of the physical factors, ADV_{O_2} and MIX_{O_2} , on the bottom O_2 is different to that for V_{sub} . While in 2002 ADV_{O_2} shows a similar effect on O_2 as for the sub-MLD O_2 , its effect in 2010 is opposite to that for V_{sub} , resulting in a minor increase of about 1.1 g O_2 m⁻². During the last 3 weeks of stratification in 2002, the same positive effect of ADV_{O_2} as in the sub-MLD mass balance is shown, initiating the recovery of the bottom O_2 before MIX_{O_2} intensifies. MIX_{O_2} has a consistently positive effect on the bottom O_2 in both years. Its integrated effect is increased relative to V_{sub} by the factor 1.7 and 1.4 in 2002 and 2010, respectively.

The relative contribution of the biological O_2 sinks in the bottom layer is also different to the sub-MLD volume. The 2000–2012 averages reveal that in the bottom layer REM_{sed} accounts for 50.1 ± 1.2 % of the total biological O_2 consumption, while REM_{pel} contributes to 32.2 ± 1.4 %. Thus, aerobic remineralisation consistently adds up to more than 80 % of the biological O_2 consumption in the bottom layer. This shift results from the different volumes considered, and the fact that REM_{sed} only has a direct effect on the deepest pelagic layer. Average O_2 consumption due to REM_{sed} results in values between 3.9 and 6.5 mmol O_2 m⁻² d⁻¹.

950 For RES_{200} , the influence on the bottom O_2 concentrations is lower than in V_{sub} ($11.3 \pm 1.2\%$ during 2000–2012). This relates to the fact that zooplankton tends to stay in the upper part of the water column where phytoplankton concentrations are higher. NIT represents the weakest sink for bottom O_2 with an average contribution of $6.4 \pm 0.6\%$ during these years. PP as a potential source for O_2 is negligible in the bottom layer due to light limitation.

955 The analysis clearly shows vertical mixing is the only efficient gain term for O_2 in the bottom layer. Benthic aerobic remineralisation constitutes the major driver for O_2 deficiency in the North Sea O_2 minimum zone, although pelagic aerobic remineralisation still has a significant effect on bottom O_2 , but accounts for a remarkably lower proportion than in the entire sub-MLD volume. The simulated benthic remineralisation rates are in the same order as
960 those derived from observations giving a range from 7 to 25 $mmol O_2 m^{-2} d^{-1}$ for a nearby station (station 3 in Upton et al., 1993), however, rather at the lower end of this range.

3.6 Spatial variability in the North Sea bottom O_2 dynamics

Figure 9a and b show the bottom O_2 mass balances of regions 4 (southern North Sea) and 5 (northern North Sea) in 2002 (see Fig. 2 for location of regions). Both regions show
965 different stratification periods than in region 3. In region 4, the period between the first and last day of stratification accounts for only 163 days compared to 187 in region 3. Additionally, stratification is temporarily intermittent in late April and early July. In region 5, stratification lasts for 211 days without any interruptions. The water depths and bottom layer volumes also differ between the regions. Region 3 has an average water depth of 47.75 m and a bottom
970 layer volume of about 14.4 km^3 , while region 4 is characterised by an average depth of 45 m and a bottom layer volume of 11.9 km^3 . Region 5 has an average bottom depth of 99.23 m and a bottom layer volume of 16.3 km^3 .

The O_2 concentrations at the beginning of the stratified period in regions 4 ($9.74 mg O_2 L^{-1}$) and 5 ($9.46 mg O_2 L^{-1}$) are lower than in region 3. In contrast, both re-
975 gions show higher concentrations at the end of stratification compared to region 3. These

values reach $6.98 \text{ mg O}_2 \text{ L}^{-1}$ in region 4 and $7.61 \text{ mg O}_2 \text{ L}^{-1}$ in region 5, compared to $6.76 \text{ mg O}_2 \text{ L}^{-1}$ in region 3.

In region 4, intense mixing in late June/early July, indicated by the steep increase in MIX_{O_2} , causes the breakdown of stratification and the complete replenishment of bottom O_2 . Integrated over the stratified period the effect of MIX_{O_2} is almost 1.5 times higher than in region 3. In region 5, MIX_{O_2} represents a significantly lower supply of O_2 , which mainly relates to the significantly greater water depth favouring more stable stratification. ADV_{O_2} has an opposite effect in regions 4 and 5 relative to region 3, however, showing only minor negative integrated effects.

The integrated biological O_2 consumption in region 4 is about 7 % less than in region 3. Referring to changes in O_2 concentrations, the consumption even exceeds that in region 3 by about 6 %, due to the thinner bottom layer, and corresponds ~~with~~ to an EXP_{org} below 25 m depth (calculation analogous to Table 1) in region 4 being 19 % higher than in region 3. In the deeper region 5, EXP_{org} accounts for 62 % of that in region 3, while biological O_2 consumption accounts for only 35 % of that in region 3.

Despite the differences in the overall biological O_2 consumption, the relative contributions of the different sink processes in region 4 are in the same order as in region 3. REM_{sed} represents the largest contributor with about 54.6 % of the total biological consumption, while REM_{pel} accounts for 27.2 %. Thus, the combined effect of REM_{sed} and REM_{pel} accounts for 81.8 % which is similar to region 3. Average daily benthic remineralisation rates are higher than in region 3 and yield $8.9 \text{ mmol O}_2 \text{ m}^{-2} \text{ d}^{-1}$. The relative contributions for RES_{200} and NIT result in 13.6 and 4.6 %, respectively.

The comparison of the relative contribution of REM_{pel} and REM_{sed} in region 5 reveals some changes compared to regions 3 and 4. REM_{sed} accounts for about 70 % of the total biological O_2 consumption, while REM_{pel} contributes to only about 20 %. This relates to the generally lower amount of ~~organic matter exported into the deeper~~ exported organic matter reaching the model bottom layer (63 % of that in region 3), ~~due to the greater bottom depth, resulting in lower concentrations of pelagic bacteria~~. On the one hand, this causes lower O_2

consumption due to REM_{pel} , and on the other hand, enhances REM_{sed} relative to REM_{pel} as more organic matter reaches the bottom.

Considering the combined effect of stratification and biological consumption in region 4 reveals that the shorter stratification period and the strong mixing prohibit the evolution of low O_2 conditions in this region, despite the highest biological consumption. The higher benthic remineralisation rate compared to region 3 underlines the high potential for low O_2 conditions in the Oyster Grounds under persistent seasonal stratification. This is in good agreement with the findings by Greenwood et al. (2010), who observed bottom O_2 concentrations less than $6 \text{ mg } O_2 \text{ L}^{-1}$ in this area. As in region 3, the simulated benthic remineralisation rate lies at the lower end of the range of 5.6 to $30.6 \text{ mmol } O_2 \text{ m}^{-2} \text{ d}^{-1}$ obtained from observational studies near this site (Lohse et al., 1996; Weston et al., 2008). This suggests that the model most likely underestimates benthic remineralisation rates.

In region 5, the ~~export of organic matter into~~ amount of exported organic matter reaching the bottom layer (deepest pelagic model layer) is limited due to the great water depth. Thus, biological consumption in the bottom layer is low, preventing the evolution of O_2 deficiency, even though stratification lasts longer and is more stable than in the other regions. This suggests that region 5 is unlikely to be affected by low bottom O_2 concentrations. However, Queste et al. (2013) found bottom O_2 concentrations of about $6 \text{ mg } O_2 \text{ L}^{-1}$ near this area in 2010, which indicates that this area can be affected by O_2 deficiency.

3.7 Interpreting observed bottom O_2 at North Dogger

The O_2 observations at station North Dogger (Greenwood et al., 2010) shown in Fig. 3a and b showed similar O_2 concentrations of about $9.5 \text{ mg } O_2 \text{ L}^{-1}$ at the beginning of the stratified period, but revealed a faster decrease in bottom O_2 during 2007 compared to 2008. As the simulation showed the same tendency with respect to the ~~inter-annual differences~~ differences between the two years, the mass balances for station North Dogger for 2007 and 2008 are presented in Fig. 10a and b, respectively, in order to interpret the observed temporal evolution of bottom O_2 .

The simulation yields an average rate of O_2 reduction during the stratified period of about $0.009 \text{ mg } O_2 \text{ L}^{-1} \text{ d}^{-1}$ in 2007, and a rate of about $0.007 \text{ mg } O_2 \text{ L}^{-1} \text{ d}^{-1}$ in 2008. The integrated effect of the physical factors, ADV_{O_2} and MIX_{O_2} , is quite similar for both years providing a gross increase in O_2 of about $16.3 \text{ g } O_2 \text{ m}^{-2}$ integrated over the stratified period. Thus, the main ~~inter-annual variations~~ variations between the two years must be related to biological factors.

The temporal evolution of the biological consumption processes is also similar in both years, with higher rates in 2007. The integrated effect of all biological sink processes results in $-40.6 \text{ g } O_2 \text{ m}^{-2}$, which corresponds ~~with~~ to an average consumption rate of $0.18 \text{ g } O_2 \text{ m}^{-2} \text{ d}^{-1}$. For 2008, the simulation yields a ~~by~~ 6.8 $\text{g } O_2 \text{ m}^{-2}$ lower biological consumption due to a $0.02 \text{ g } O_2 \text{ m}^{-2} \text{ d}^{-1}$ lower consumption rate. This constitutes a relative difference of 13% between the two years. For EXP_{org} below 25 m depth during summer (calculation analogous to Table 1), the same relative difference is found.

The relative contribution of the different processes to the overall bottom O_2 consumption shows only minor changes between the two years. In both years REM_{sed} accounts for about 58%, while REM_{pel} accounts for about 31%. RES_{zoo} and NIT contribute to about 3 and 8% in both years, respectively. This shows that ~~inter-annual~~ the variations between 2007 and 2008 at North Dogger are mainly driven by differences in the organic matter export. The steeper decrease in bottom O_2 in 2007 results from the enhanced supply of organic matter and the subsequent increased degradation by bacteria. The enhanced release of ammonium due to pelagic and benthic remineralisation consequently triggers an increase in nitrification.

In contrast to the findings by Greenwood et al. (2010), who argued that the relatively strong advection at North Dogger may ventilate the bottom layers in terms of O_2 , our results suggest that advection only has a minor positive effect due to the only slightly higher O_2 concentrations in the surrounding waters. The large contribution of bacterial remineralisation (REM_{sed} and REM_{pel}) accounting for almost 90% of the overall biological consumption at station North Dogger confirms that the estimates for C remineralisation rates made by Greenwood et al. (2010) provide reasonable results. However, as NIT also accounts

1060 for about 8% of the total biological O₂ consumption, this process should be considered to obtain more precise estimates for C remineralisation rates.

4 Conclusions and perspectives

1065 The North Sea is one of the shelf regions regularly experiencing seasonal O₂ deficiency in the bottom water (Diaz and Rosenberg, 2008; Emeis et al., 2015; Rabalais et al., 2010). However, not all areas of the North Sea are similarly affected by low O₂ conditions (e.g., Queste et al., 2013) due to different characteristics with respect to stratification and O₂ consumption. Observations and model results suggest that the area between 54–57° N and 4.5–7° E shows the highest potential for low O₂ conditions, but also areas around the Doggerbank experience lowered bottom O₂ concentrations.

1070 The model-based analysis of different factors affecting O₂ (~~Sect. 3.3~~) showed that besides sufficiently long stratification (> 60 days), ~~the upper surface~~ layer primary production (driving organic matter export) and ~~the~~ sub-thermocline volume are the key parameters influencing the bottom O₂ evolution. Based on this, the North Sea can be subdivided into three different zones in terms of O₂ dynamics: (1) a highly productive, non-stratified coastal zone (region A), (2) a productive, seasonally stratified zone with a small sub-thermocline volume (region B), and (3) a productive, seasonally stratified zone with a large sub-thermocline volume (regions C and D). While the zones of type 1 and 3 are unlikely to be affected by low O₂ conditions due to either continuously ongoing ventilation (type 1) or the large sub-thermocline volume ~~damping diluting~~ the effect of O₂ consumption (type 3), type 2 is highly susceptible to low O₂ conditions. This results from the specific combination of high upper layer productivity and small sub-thermocline volume, which causes a strong impact of the consumption processes on the decrease in the bottom O₂ concentrations.

1080 The ~~presented ODI approach ODI~~ demonstrates that this regional characterisation, based on only three controlling parameters, can be applied to most parts of the North Sea. The ~~strong link between upper layer primary production and organic matter export allowed for the further simplification. Similarly, the bottom depth can be used as a proxy for~~

1090 the sub-thermocline volume. Consequently, the ODI is less complex in comparison ODI is rather simple compared to the eutrophication risk index (EUTRISK; Druon et al., 2004) ; ~~which intends to directly map bottom concentrations. In contrast, the ODI as it is designed~~ to indicate regions with higher risk for O₂ deficiency. ~~As the definition of the ODI is based on parameters which are easily accessible, the ODI~~ Therefore, it may also allow for an operational use as the information on stratification can be derived from operational hydrodynamical models and information on net primary production from satellite data.

1095 ~~While the regional characteristic and the ODI only provide a qualitative picture of the North Sea dynamics, the model-derived mass balances allowed for the quantification of the governing processes and their inter-annual and spatial variability. Inter-annual variations in the sub-thermocline and bottom evolution are mainly driven by differences in the upper layer primary productivity. This supports the choice of net primary production as a proxy for the organic matter export in the ODI definition, and its stronger weighting therein.~~ In addition, the mass balances revealed how the different direct and indirect effects of primary productivity influence the dynamics. Increased primary productivity enhances the export of dead phytoplankton into the deeper layers. Furthermore, it enhances zooplankton growth which causes an additional increase in organic matter production and export. This enhanced zooplankton growth further increases consumption due to respiration. The overall increase in organic matter export results in stronger bacterial remineralisation which in turn triggers nitrification due to the stronger release of ammonium.

1100 ~~The mass balances also~~ The model-based mass balances showed that pelagic bacterial remineralisation constitutes the largest O₂ consuming process within the sub-thermocline volume, ~~thus, it is crucial for the supply from the mid-water into the bottom layer.~~ In the bottom layer, benthic remineralisation constitutes the major O₂ sink, which consistently contributes ~~to more than 50 % of to~~ the overall bottom O₂ consumption ~~and shows an increasing relative contribution with increasing bottom depth. In contrast, pelagic remineralisation is characterised by a decreasing influence in deeper regions as organic matter concentrations within the pelagic bottom layer are lower in greater depth. Its relative contribution to~~. Pelagic remineralisation consistently contributes to more than 20 % of the overall bot-

tom O_2 consumption ~~consistently exceeds 20~~. ~~The effect of zooplankton respiration varies between almost no effect in deep regions and~~. ~~Zooplankton respiration and nitrification are less important, however, can contribute to up to 14 % in shallower areas, whereas nitrification shows only minor variations in its relative contribution (3–8 and 8 %)~~. ~~Besides this, respectively. In addition~~, the results suggest that the relative contribution of the different O_2 consuming processes in the bottom layer at a certain location depends on the water column depth and is independent of the overall consumption.

~~In contrast to the interpretation of~~ ~~The mass balances also showed that differences in the surface layer primary production drive variations in the sub-thermocline and bottom~~ O_2 ~~measurements by Queste et al. (2013), who proposed that events of mixing and /or advection of oxygenated water are likely to positively affect the bottom evolution between different years. Increased primary production directly enhances the export of dead phytoplankton into the deeper layers. Furthermore, it enhances zooplankton growth which causes an additional increase in organic matter production and export. This enhanced zooplankton growth further increases~~ O_2 ~~concentrations, our consumption due to respiration. The overall increase in organic matter export results in stronger bacterial remineralisation which in turn triggers nitrification due to the stronger release of ammonium.~~

~~Our~~ analysis suggests that advection usually only has a minor effect on the bottom O_2 dynamics in most North Sea regions ~~which contradicts the interpretation by Queste et al. (2013)~~. However, during years of especially low bottom O_2 concentrations it may play an important role for the recovery of the O_2 levels ~~at the end of the stratified period, even before stratification breaks down and vertical mixing replenishes the bottom concentrations before the breakdown of stratification in autumn~~. In addition, we showed that during the summer period only very strong mixing results in a net increase in O_2 as the enhanced nutrient supply triggers primary production, eventually increasing the biological O_2 consumption, which balances or even exceeds the enhanced O_2 supply.

~~The qualitative characterisation and the detailed quantitative analysis demonstrates the potential of ecosystem models to describe~~ ~~This study demonstrated that ecosystem models~~

1145 are capable of describing the key features of the O₂ dynamics as an integral part of the
North Sea ecosystem. ~~In This, in~~ combination with the provision of a spatially and tempo-
rally consistent picture, ~~this is a strong benefit compared to one-dimensional model studies~~
(e.g., Meire et al., 2013). ~~With the capability to describe the temporal evolution and spatial~~
1150 ~~patterns of bottom, ecosystem models can be used to obtain a more detailed picture of~~
~~the spatial extent and duration of low conditions. This~~ is useful for the detection of re-
gions susceptible to low O₂ conditions which therefore require enhanced management;
~~and~~. Additionally, this is of importance for monitoring authorities as our model showed that
~~temporal variability in late-summer bottom O₂ is small implying that measurements taken~~
1155 ~~during this period provide a~~ measurements taken in late summer provide a synoptic picture
of the North Sea O₂ conditions.

~~In addition, three-dimensional models can provide valuable insight in the dynamics in~~
~~the context of the natural variability of the ecosystem. This can be related to weather~~
~~conditions which result in different stratification patterns of the North Sea, or in variations~~
~~in the biological production. The latter can be induced by anthropogenic drivers, such as~~
1160 ~~increased atmospheric deposition (Troost et al., 2013) or riverine nutrient input as shown~~
~~for the exceptionally wet year 2002 (Lenhart et al., 2010). Thus, ecosystem models can~~
~~help to estimate the impact of these anthropogenic impacts on the bottom in offshore areas~~
~~which are susceptible to deficiency.~~

This study is focused on the general characterisation of the key factors driving the North
1165 ~~Sea dynamics and a description and~~ This study provides a general characterisation and
process-based analysis of the North Sea ~~ecosystem~~-O₂ dynamics in its present state, in-
cluding the actual eutrophication status in the “continental coastal region” as defined for
the OSPAR assessment (Claussen et al., 2009). The question on the anthropogenic ~~part~~
~~of contribution to~~ the O₂ deficiency problem in relation to elevated ~~river loads~~ nutrient
1170 supply is beyond the scope of this study ~~and would require additional model scenarios~~
~~taking into account pristine conditions without any anthropogenic contribution (Serna et al.,~~
~~2010). Besides the determination of the anthropogenic contribution, further studies are~~
~~needed to investigate the cause-effect relationship between the effect of the discharges~~

1175 of inorganic nutrients and organic matter by the rivers (Topcu and Brockmann, 2015).
Kemp et al. (2009) analysed the success of restoring different ecosystems with and without
taking into account the organic matter input by rivers. Based on our findings on the
processes dominating the bottom. However, the capability of three-dimensional models to
describe the O_2 evolution, such studies would allow managers to make informed decisions
about necessary management measures. dynamics in the context of the natural variability
1180 of the ecosystem can be related to changes in anthropogenic drivers, such as increased
atmospheric deposition (Troost et al., 2013) or riverine nutrient input (Lenhart et al., 2010).

This assessment can be extended towards new measures to combat eutrophication
Similar model studies are essential for the assessment within the Water Framework
1185 Directive (WFD), in which dissolved O_2 plays an important role as one of the five
“General chemical and physiochemical elements supporting the biogeological elements”
for assessment is used as a key parameter (Best et al., 2007). As the WFD assessment
depends strongly on the description of pristine conditions, related to natural nutrient levels
(Topcu et al., 2009), ecosystem models can provide insight in the a consistent picture of the
1190 North Sea O_2 dynamics under these pristine conditions, and in addition, for the application
of the WFD measures (Schernewski et al., 2015) on the North Sea. Even though and of
the effects of WFD reductions (Schernewski et al., 2015). As river load reductions within
the WFD regulation is applied only to a narrow band along the coastline, the question of
how nutrient reductions under WFD measures will effect affect the entire North Sea ecosys-
1195 tem, also in terms of bottom O_2 conditions, is highly relevant. Therefore, is one of the main
descriptors under these scenarios can also be interpreted within the frame of the Marine
Framework Directive (MSFD), which involves O_2 as one of the main descriptors for the
definition of the “Good Environmental Status” as the target condition.

The article on the “spreading dead zones” by Diaz and Rosenberg (2008) resulted
1200 in an increased public awareness of Recent observational studies explicitly highlight
the importance of organic nutrient loads on the O_2 deficiency, also dynamics in the
context of nutrient reductions (Kemp et al., 2009; Topcu and Brockmann, 2015). Thus,

1205 ~~future modelling studies on the effects of nutrient reductions on the debate on climate change. One can start the discussion with the straight forward argument that climate change scenarios show an earlier onset and increased intensity of stratification for the North Sea due to increasing temperatures (Lowe et al., 2009; Meire et al., 2013). Mathis and Pohlmann (2014) also found an increase in the water temperatures of marine environment should differentiate between the effects of organic and inorganic nutrient inputs in order to optimise measures in the catchment area with respect to cost efficiency.~~

1210 Diaz and Rosenberg (2008) report an exponential expansion of global O₂ deficiency (and hypoxia) since the 1960s and argue that future changes in O₂ conditions will strongly depend on the effects of climate change on stratification and riverine nutrient supply. For the North Sea, however, accompanied by ~~aweakening of stratification which would support enhanced ventilation of the bottom water. The increase in temperature will decrease several model studies predict a rise in water temperature (e.g., Lowe et al., 2009; Meire et al., 2013; Mathis and Pohlmann, 2014) which will reduce the O₂ solubility in the bottom layer (Weston et al., 2008). Changes in the weather conditions, such as increased precipitation or other extreme events (Rabalais et al., 2010), could furthermore lead to increased nutrient loads triggering higher primary production which could increase the risk of low (Weston et al., 2008). Stratification intensity may either increase (Lowe et al., 2009; Meire et al., 2013) or even decrease (Mathis and Pohlmann, 2014), implying opposed effects on bottom O₂. Primary production could increase due to enhanced nutrient supply caused by changes in weather conditions (Rabalais et al., 2010) or due to a temperature-driven increase in metabolic rates (van der Molen et al., 2013), which could eventually aggravate the O₂ conditions (Justić et al., 2003). In contrast, Gröger et al. (2013) predicted a North Sea wide reduction in primary production by about 30 % due to reduced winter nutrient import from the Atlantic. Another potential impact was argued by van der Molen et al. (2013), who concluded that the temperature-driven increase in metabolic rates and nutrient cycling will be followed by an increase in primary production. In combination with an increase in the benthic~~

1225

1230

~~metabolic rates and other constraints, this will eventually lead to a decrease in the bottom concentrations.~~

As these potential changes in the O_2 conditions will also affect the biocoenosis of the North Sea (Emeis et al., 2015), it is important to foster the analysis of potential impacts of climate change and changes in nutrient loads on the O_2 dynamics. ~~This study provided evidence that ecosystem models can contribute to the better understanding of the complex interplay of hydrodynamical and biogeochemical processes controlling the bottom dynamics in the North Sea. This study showed that ecosystem models can be used to either interpret in-situ measurements, or to estimate the impact of climate change or nutrient reduction scenarios with respect to deficiency and its concomitants. Thus, they can provide relevant information for the ecological management of marine coastal ecosystems.~~

Data availability

The time series data from the Cefas SmartBuoy programme can be accessed via: <http://cefasmapping.defra.gov.uk/Smartbuoy>. The time series data of BSH MARNET programme can be accessed via: http://www.bsh.de/en/Marine_data/Observations/MARNET_monitoring_network/. The spatially resolved data from the North Sea cruises 2001, 2005 and 2008 have been released in the framework of the EU-FP6 project CARBOOCEAN and can be accessed via: <http://dataportal.carboocean.org/>.

Appendix A: Evaluation of the stratification and MLD criterion

Figure A1 shows the Hovmöller diagram of simulated T at station North Dogger (see Fig. 2, region 2) for the year 2007, including the MLD (dashed magenta line) derived from the simulated T field according to Eqs. (1) and (2). Regarding the onset of stratification in late March it is shown, that the near-surface ~~T (down to 25 (0–25 m) T~~ starts to increase relatively to ~~the T in the deeper layers. The $T_{crit} = 0.5 K$ is reached on 26 April, marking the~~ beginning of the stratified period ~~on 26 April coincides very well with this slowly evolving separation of surface and bottom waters according to Eq. (1).~~ The maximum vertical T gradient at the

onset occurs in 25 m depth. From that moment stratification according to Eq. (1) persists until 31 October, which may represent a slight overestimation as the maximum T gradient is found in 60 m depth already, indicating deep mixing.

1260 During the first two months of the stratified period (April/May) the MLD shows stronger fluctuations in terms of its actual depth. This results from the relatively weak near-surface stratification, and thus, the stronger effect of mainly wind-induced mixing reaching depths of up to 35 m. These events are indicated by the episodic increase and decrease of surface T . From early June to end of July, the MLD is less variable in depth due to the persistent
1265 surface heating and less strong wind events. In late June a short-term decrease in surface T indicating enhanced mixing occurs which also results in a deepening of the MLD. From August until the end of the stratified period the MLD shows a deepening trend which is caused by the decreasing surface heating and increasing wind activity.

1270 The main assumption behind the rather small critical T difference of 0.05 K is, that even if the surface mixed layer is interrupted due to mixing, this does not necessarily result in a complete overturning of the water column. Thus, even a minor difference in T indicates a bottom layer unaffected from vertical mixing. Despite this significant difference to common MLD criteria (e.g Kara et al., 2000, therein Table 1), the criterion applied in this study represents the stratification conditions quite well. However, it should be noted that the end
1275 of the stratified period may be slightly overestimated. In addition, in regions with a less pronounced onset of stratification, i.e., a less distinct increase in surface T , the determined timing of the onset may be slightly too early. The use of the maximum T gradient to determine the MLD under stratified conditions yields reasonable results, and is closely related to real conditions as the thermocline is defined as the layer with the maximum T gradient.

1280 *Acknowledgements.* We would like to thank Sonja van Leeuwen from Cefas for providing updated data on freshwater and nutrient loads for the major rivers across Europe. We further thank Jerzy Bartnicki for providing atmospheric nitrogen deposition data from the European Monitoring and Evaluation Programme (EMEP). We thank Dilek Topcu and Uwe Brockmann from the University of Hamburg for providing the map of observed O_2 deficiency in the North Sea. Furthermore, we
1285 thank the editor Veronique Garçon and two anonymous referees for the valuable comments and constructive criticism, which helped to significantly improve the manuscript. The model simulation was conducted on Blizzard, the IBM Power6 mainframe at the German Climate Computing Centre

(DKRZ) in Hamburg. The North Sea sampling in 2001, 2005 and 2008 was supported by the Dutch Science Foundation (NWO), CARBOOCEAN (EU-FP6) and the Royal Netherlands Institute for Sea Research (NIOZ). Cefas SmartBuoy data were collected under the UK Department for Environment, Food and Rural Affairs (Defra) contract ME3205 (Marine Ecosystems Connections: essential indicators of healthy, productive and biologically diverse seas). Markus Kreuz was partly financially supported by the Cluster of Excellence “CliSAP” (EXC177), University of Hamburg, funded by the German Science Foundation (DFG). This study was supported by the German Environmental Protection Agency (UBA) in Dessau, in the frame of the project “Implementation of Descriptor 5 Eutrophication to the MSFD”, SN: 3713225221. The publication costs were covered by Thomas Ludwig (Scientific Computing, University of Hamburg) and “CliSAP”.

References

- Arakawa, A. and Lamb, V.: Computational design of the basic dynamical processes of the UCLA general circulation model, *Methods in Computational Physics*, 17, 173–265, 1977.
- Azam, F., Fenchel, T., Field, J., Gray, J., Meyer-Reil, L., and Thingstad, F.: The ecological role of water-column microbes in the sea, *Mar. Ecol.-Prog. Ser.*, 10, 257–263, doi:10.3354/meps010257, 1983.
- Backhaus, J.: A three-dimensional model for the simulation of shelf sea dynamics, *Deutsche Hydrografische Zeitschrift*, 38, 165–187, doi:10.1007/BF02328975, 1985.
- Backhaus, J. and Hainbucher, D.: A finite difference general circulation model for shelf seas and its application to low frequency variability on the North European Shelf, *Elsev. Oceanogr. Serie*, 45, 221–244, doi:10.1016/S0422-9894(08)70450-1, 1987.
- Benson, B. and Krause, D.: The concentration and isotopic fractionation of oxygen dissolved in freshwater and seawater in equilibrium with the atmosphere, *Limnol. Oceanogr.*, 29, 620–632, doi:10.4319/lo.1984.29.3.0620, 1984.
- Best, M., Wither, A., and Coates, S.: Dissolved oxygen as a physico-chemical supporting element in the Water Framework Directive, *Mar. Pollut. Bull.*, 55, 53–64, doi:10.1016/j.marpolbul.2006.08.037, 2007.
- Bozec, Y., Thomas, H., Elkalay, K., and de Baar, H.: The continental shelf pump for CO₂ in the North Sea – evidence from summer observation, *Mar. Chem.*, 93, 131–147, doi:10.1016/j.marchem.2004.07.006, 2005.

- 1320 Bozec, Y., Thomas, H., Schiettecatte, L.-S., Borges, A., Elkalay, K., and de Baar, H.: Assessment of the processes controlling the seasonal variations of dissolved inorganic carbon in the North Sea, *Limnol. Oceanogr.*, 51, 2746–2762, doi:10.4319/lo.2006.51.6.2746, 2006.
- Brockmann, U. and Eberlein, K.: River input of nutrients into the German Bight, in: *The Role of Freshwater Outflow in Coastal Marine Ecosystems*, Springer, Berlin Heidelberg, 231–240, available at: http://link.springer.com/chapter/10.1007/978-3-642-70886-2_15, accessed 29 June 2015, 1986.
- 1325 Brockmann, U. and Topcu, D.: Confidence rating for eutrophication assessments, *Mar. Pollut. Bull.*, 82, 127–136, doi:10.1016/j.marpolbul.2014.03.007, 2014.
- Brockmann, U., Billen, G., and Gieskes, W.: North Sea nutrients and eutrophication, in: *Pollution of the North Sea*, Springer, Berlin Heidelberg, 348–389, available at: http://link.springer.com/chapter/10.1007/978-3-642-73709-1_20, accessed 29 June 2015 1988.
- 1330 Brockmann, U., Laane, R., and Postma, J.: Cycling of nutrient elements in the North Sea, *Neth. J. Sea Res.*, 26, 239–264, doi:10.1016/0077-7579(90)90092-U, 1990.
- Burt, W., Thomas, H., Pätsch, J., Omar, A., Schrum, C., Daewel, U., Brenner, H., and de Baar, H.: Radium isotopes as a tracer of sediment-water column exchange in the North Sea, *Global Biogeochem. Cy.*, 28, 786–804, doi:10.1002/2014GB004825, 2014.
- 1335 Chen, X., Liu, C., O'Driscoll, K., Mayer, B., Su, J., and Pohlmann, T.: On the nudging terms at open boundaries in regional ocean models, *Ocean Model.*, 66, 14–25, doi:10.1016/j.ocemod.2013.02.006, 2013.
- Chen, X., Dangendorf, S., Narayan, N., O'Driscoll, K., Tsimplis, M., Su, J., Mayer, B., and Pohlmann, T.: On sea level change in the North Sea influenced by the North Atlantic Oscillation: local and remote steric effects, *Estuar. Coast. Shelf S.*, 151, 186–195, doi:10.1016/j.ecss.2014.10.009, 2014.
- 1340 Claussen, U., Zevenboom, W., Brockmann, U., Topcu, D., and Bot, P.: Assessment of the eutrophication status of transitional, coastal and marine waters within OSPAR, *Hydrobiologia*, 629, 49–58, doi:10.1007/s10750-009-9763-3, 2009.
- Conkright, M.E., Locarnini, R.A., Garcia, H.E., O'Brien, T.D., Boyer, T.P., Stephens, C., Antonov, J.I.: *World Ocean Atlas 2001: objective analyses, data statistics and figures CD-ROM documentation*, National Oceanographic Data Center Internal Report, National Oceanographic Data Center, Silver Spring, MD, 17, 2002.
- 1345 de Jong, F.: *Marine Eutrophication in Perspective: On the Relevance of Ecology for Environmental Policy*, Springer Science and Business Media, Berlin Heidelberg, 2006.

- 1350 Diaz, R. and Rosenberg, R.: Spreading dead zones and consequences for marine ecosystems, *Science*, 321, 926–929, doi:10.1126/science.1156401, 2008.
- Druon, J.-N., Schrimpf, W., Dobricic, S., and Stips, A.: Comparative assessment of large-scale marine eutrophication: North Sea area and Adriatic Sea as case studies, *Mar. Ecol.-Prog. Ser.*, 272, 1–23, 2004.
- 1355 Ducrotoy, J., Elliott, M., and de Jonge, V.: The North Sea, *Mar. Pollut. Bull.*, 41, 5–23, doi:10.1016/S0025-326X(00)00099-0, 2000.
- Emeis, K.-C., van Beusekom, J., Callies, U., Ebinghaus, R., Kannen, A., Kraus, G., Kröncke, I., Lenhart, L., Lorkowski, I., Matthias, V., Möllmann, C., Pätsch, J., Scharfe, M., Thomas, H., Weisse, R., and Zorita, Z.: The North Sea – a shelf sea in the Anthropocene, *J. Marine Syst.*, 141, 18–33, doi:10.1016/j.jmarsys.2014.03.012, 2015.
- 1360 Friedrich, J., Janssen, F., Aleynik, D., Bange, H. W., Boltacheva, N., Çagatay, M. N., Dale, A. W., Etiop, G., Erdem, Z., Geraga, M., Gilli, A., Gomoiu, M. T., Hall, P. O. J., Hansson, D., He, Y., Holtappels, M., Kirf, M. K., Kononets, M., Konovalov, S., Lichtschlag, A., Livingstone, D. M., Marinaro, G., Mazlumyan, S., Naeher, S., North, R. P., Papatheodorou, G., Pfannkuche, O., Prien, R., Rehder, G., Schubert, C. J., Soltwedel, T., Sommer, S., Stahl, H., Stanev, E. V., Teaca, A., Tenberg, A., Waldmann, C., Wehrli, B., and Wenzhöfer, F.: Investigating hypoxia in aquatic environments: diverse approaches to addressing a complex phenomenon, *Biogeosciences*, 11, 1215–1259, doi:10.5194/bg-11-1215-2014, 2014.
- Greenwood, N., Parker, E. R., Fernand, L., Sivyer, D. B., Weston, K., Painting, S. J., Kröger, S., 1370 Forster, R. M., Lees, H. E., Mills, D. K., and Laane, R. W. P. M.: Detection of low bottom water oxygen concentrations in the North Sea; implications for monitoring and assessment of ecosystem health, *Biogeosciences*, 7, 1357–1373, doi:10.5194/bg-7-1357-2010, 2010.
- Gröger, M., Maier-Reimer, E., Mikolajewicz, U., Moll, A., and Sein, D.: NW European shelf under climate warming: implications for open ocean – shelf exchange, primary production, and carbon absorption, *Biogeosciences*, 10, 3767–3792, doi:10.5194/bg-10-3767-2013, 2013.
- 1375 Heath, M., Edwards, A., Pätsch, J., and Turrell, W.: Modelling the Behaviour of Nutrients in the Coastal Waters of Scotland, Scottish Executive Central Research Unit, Edinburgh, 2002.
- Jickells, T.: Nutrient biogeochemistry of the coastal zone, *Science*, 281, 217–222, doi:10.1126/science.281.5374.217, 1998.
- 1380 Justić, D., Turner, R., and Rabalais, N.: Climatic influences on riverine nitrate flux: implications for coastal marine eutrophication and hypoxia, *Estuaries*, 26, 1–11, doi:10.1007/BF02691688, 2003.

- 1385 Kalnay, E., Kanamitsu, M., Kistler, R., Collins, W., Deaven, D., Gandin, L., Iredell, M., Saha, S., White, G., Woollen, J., Zhu, Y., Chelliah, M., Ebisuzaki, W., Higgins, W., Janowiak, J., Mo, K., Ropelewski, C., Wang, J., Leetmaa, A., Reynolds, R., Jenne, R., and Joseph, D.: The NCEP/NCAR 40-year reanalysis project, *B. Am. Meteorol. Soc.*, 77, 437–471, doi:10.1175/1520-0477(1996)077<0437:TNYRP>2.0.CO;2, 1996.
- Kara, A., Rochford, P., and Hurlburt, H.: An optimal definition for ocean mixed layer depth, *J. Geophys. Res.-Oceans*, 105, 16803–16821, doi:10.1029/2000JC900072, 2000.
- 1390 Kemp, W. M., Testa, J. M., Conley, D. J., Gilbert, D., and Hagy, J. D.: Temporal responses of coastal hypoxia to nutrient loading and physical controls, *Biogeosciences*, 6, 2985–3008, doi:10.5194/bg-6-2985-2009, 2009.
- Kistler, R., Collins, W., Saha, S., White, G., Woollen, J., Kalnay, E., Chelliah, M., Ebisuzaki, W., Kanamitsu, M., Kousky, V., van den Dool, H., Jenne, R., and Fiorino, M.: The NCEP-NCAR 50-year reanalysis: monthly means CD-ROM and documentation, *B. Am. Meteorol. Soc.*, 82, 247–267, doi:10.1175/1520-0477(2001)082<0247:TNNYRM>2.3.CO;2, 2001.
- 1395 Kröncke, I. and Knust, R.: The Dogger Bank: a special ecological region in the central North Sea, *Helgol. Mar. Res.*, 49, 335–353, doi:10.1007/BF02368361, 1995.
- Lenhart, H.-J. and Pohlmann, T.: The ICES-boxes approach in relation to results of a North Sea circulation model, *Tellus A*, 49, 139–160, doi:10.1034/j.1600-0870.1997.00010.x, 1997.
- 1400 Lenhart, H.-J., Mills, D., Baretta-Bekker, H., van Leeuwen, S., van der Molen, J., Baretta, J., Blaas, M., Desmit, X., Kühn, W., Lacroix, G., Los, H., Ménesguen, A., Neves, R., Proctor, R., Ruardij, P., Skogen, M., Vanhoute-Brunier, A., Villars, M., and Wakelin, S.: Predicting the consequences of nutrient reduction on the eutrophication status of the North Sea, *J. Marine Syst.*, 81, 148–170, doi:10.1016/j.jmarsys.2009.12.014, 2010.
- 1405 Lohse, L., Kloosterhuis, H., van Raaphorst, W., and Helder, W.: Denitrification rates as measured by the isotope pairing method and by the acetylene inhibition technique in continental shelf sediments of the North Sea, *Mar. Ecol.-Prog. Ser.*, 132, 169–179, 1996.
- Lorkowski, I., Pätsch, J., Moll, A., and Kühn, W.: Interannual variability of carbon fluxes in the North Sea from 1970 to 2006 – Competing effects of abiotic and biotic drivers on the gas-exchange of CO₂, *Estuar. Coast. Shelf S.*, 100, 38–57, doi:10.1016/j.ecss.2011.11.037, 2012.
- 1410 Lowe, J., Howard, T., Pardaens, A., Tinker, J., Holt, J., Wakelin, S., Milne, G., Leake, J., Wolf, J., Horsburgh, K., Reeder, T., Jenkins, G., Ridley, J., Dye, S., and Bradley, S.: UK Climate Projections Science Report: Marine and Coastal Projections, Tech. rep., Met Office Hadley Centre, Exeter, UK, available at: <http://nora.nerc.ac.uk/9734/>, accessed 29 June 2015, 2009.

- 1415 Mathis, M., and Pohlmann, T.: Projection of physical conditions in the North Sea for the 21st century. *Clim. Res.*, 61, 1–17, doi:doi:10.3354/cr01232, 2014.
- Meire, L., Soetaert, K. E. R., and Meysman, F. J. R.: Impact of global change on coastal oxygen dynamics and risk of hypoxia, *Biogeosciences*, 10, 2633–2653, doi:10.5194/bg-10-2633-2013, 2013.
- 1420 Mills, D. K., Greenwood, N., Kröger, S., Devlin, M., Sivyer, D. B., Pearce, D., Cutchey, S., and Malcolm, S.: New approaches to improve the detection of eutrophication in UK coastal waters, *Environ Res Eng Manag*, 2 (32), 36–42, 2005.
- Müller, L.: Sauerstoffdynamik der Nordsee – Untersuchungen mit einem drei-dimensionalen Ökosystemmodell (in German only), *Berichte des BSH*, 43, 1–171., 2008.
- 1425 Neumann, T.: Towards a 3D-ecosystem model of the Baltic Sea, *J. Marine Syst.*, 25, 405–419, doi:10.1016/S0924-7963(00)00030-0, 2000.
- O’Boyle, S. and Nolan, G.: The influence of water column stratification on dissolved oxygen levels in coastal and shelf waters around Ireland, *Biol. Environ.*, 110B, 195–209, doi:10.3318/BIOE.2010.110.3.195, 2010.
- 1430 O’Driscoll, K., Mayer, B., Ilyina, T., and Pohlmann, T.: Modelling the cycling of persistent organic pollutants (POPs) in the North Sea system: fluxes, loading, seasonality, trends, *J. Marine Syst.*, 111, 69–82, doi:10.1016/j.jmarsys.2012.09.011, 2013.
- OSPAR-Commission: OSPAR integrated report 2003 on the eutrophication status of the OSPAR maritime area based upon the first application of the Comprehensive Procedure, London, 2003.
- 1435 OSPAR-Commission: Common procedure for the identification of the eutrophication status of the OSPAR maritime area, London, 2005.
- Otto, L., Zimmerman, J., Furnes, G., Mork, M., Saetre, R., and Becker, G.: Review of the physical oceanography of the North Sea, *Neth. J. Sea Res.*, 26, 161–238, doi:10.1016/0077-7579(90)90091-T, 1990.
- 1440 Pätsch, J. and Kühn, W.: Nitrogen and carbon cycling in the North Sea and exchange with the North Atlantic – a model study. Part I. Nitrogen budget and fluxes, *Cont. Shelf Res.*, 28, 767–787, doi:10.1016/j.csr.2007.12.013, 2008.
- Pingree, R., Holligan, P., and Mardell, G.: The effects of vertical stability on phytoplankton distributions in the summer on the northwest European Shelf, *Deep-Sea Res.*, 25, 1011–1016, doi:10.1016/0146-6291(78)90584-2, 1978.
- 1445 Pohlmann, T.: Untersuchung hydro- und thermodynamischer Prozesse in der Nordsee mit einem dreidimensionalen numerischem Modell, *Berichte aus dem Zentrum für Meeres- und Kli-*

maforschung, Reihe B, Zentrum für Meeres- und Klimaforschung der Universität Hamburg, Hamburg, 1–116, 1991.

1450 Pohlmann, T.: Predicting the thermocline in a circulation model of the North Sea – Part I: model description, calibration and verification, *Cont. Shelf Res.*, 16, 131–146, doi:10.1016/0278-4343(95)90885-S, 1996.

1455 Queste, B., Fernand, L., Jickells, T., and Heywood, K.: Spatial extent and historical context of North Sea oxygen depletion in August 2010, *Biogeochemistry*, 113, 53–68, doi:10.1007/s10533-012-9729-9, 2013.

Rabalais, N. N., Díaz, R. J., Levin, L. A., Turner, R. E., Gilbert, D., and Zhang, J.: Dynamics and distribution of natural and human-caused hypoxia, *Biogeosciences*, 7, 585–619, doi:10.5194/bg-7-585-2010, 2010.

1460 Rachor, E. and Albrecht, H.: Sauerstoff-Mangel im Bodenwasser der Deutschen Bucht, *Veröff. Inst. Meeresforsch. Bremerh.*, 19, 209–227, 1983.

Reinthalder, T., Bakker, K., Manuela, R., Van Ooijen, J., and Herndl, G.: Fully automated spectrophotometric approach to determine oxygen concentrations in seawater via continuous-flow analysis, *Limnol. Oceanogr.-Meth.*, 4, 358–366, doi:10.4319/lom.2006.4.358, 2006.

1465 Salt, L., Thomas, H., Prowe, A., Borges, A., Bozec, Y., and de Baar, H.: Variability of North Sea pH and CO₂ in response to North Atlantic Oscillation forcing, *J. Geophys. Res.-Biogeo.*, 118, 1584–1592, doi:10.1002/2013JG002306, 2013.

Schernewski, G., Friedland, R., Carstens, M., Hirt, U., Leujak, W., Nausch, G., Neumann, T., Petenati, T., Sagert, S., Wasmund, N., and von Weber, M.: Implementation of European marine policy: new water quality targets for German Baltic waters, *Mar. Policy*, 51, 305–321, doi:10.1016/j.marpol.2014.09.002, 2015.

1470 Schöpp, W., Posch, M., Mylona, S., and Johansson, M.: Long-term development of acid deposition (1880–2030) in sensitive freshwater regions in Europe, *Hydrol. Earth Syst. Sci.*, 7, 436–446, doi:10.5194/hess-7-436-2003, 2003.

1475 Seitzinger, S. and Giblin, A.: Estimating denitrification in North Atlantic continental shelf sediments, *Biogeochemistry*, 35, 235–260, 1996.

~~Serna, A., Pätsch, J., Dähnke, K., Wiesner, M. G., Hass, H. C., Zeiler, Z., Hebbeln, D. and Emeis, K.-C.: History of anthropogenic nitrogen input to the German Bight/SE North Sea as reflected by nitrogen isotopes in surface sediments, sediment cores and hindcast models, *Cont. Shelf Res.*, 30(15), 1626–1638, doi:10.1016/j.csr.2010.06.010, 2010.~~

- 1480 Steele, J.: Environmental control of photosynthesis in the sea, *Limnol. Oceanogr.*, 7, 137–150, doi:10.4319/lo.1962.7.2.0137, 1962.
- Taylor, K.: Summarizing multiple aspects of model performance in a single diagram, *J. Geophys. Res.-Atmos.*, 106, 7183–7192, 2001.
- 1485 Thomas, H., Bozec, Y., Elkalay, K., de Baar, H. J. W., Borges, A. V., and Schiettecatte, L.-S.: Controls of the surface water partial pressure of CO₂ in the North Sea, *Biogeosciences*, 2, 323–334, doi:10.5194/bg-2-323-2005, 2005.
- Topcu, H.D. and Brockmann, U.H.: Seasonal oxygen depletion in the North Sea, a review, *Mar. Pollut. Bull.*, doi:10.1016/j.marpolbul.2015.06.021, 2015.
- 1490 Topcu, D., Brockmann, U., and Claussen, U.: Relationship between eutrophication reference conditions and boundary settings considering OSPAR recommendations and the Water Framework Directive – examples from the German Bight, *Hydrobiologia*, 629, 91–106, doi:10.1007/s10750-009-9778-9, 2009.
- 1495 Troost, T., Blaas, M., and Los, F.: The role of atmospheric deposition in the eutrophication of the North Sea: a model analysis, *J. Marine Syst.*, 125, 101–112, doi:10.1016/j.jmarsys.2012.10.005, 2013.
- Upton, A., Nedwell, D., Parkes, R., and Harvey, S.: Seasonal benthic microbial activity in the southern North Sea; oxygen uptake and sulphate reduction, *Mar. Ecol.-Prog. Ser.*, 101, 273–281, doi:10.3354/meps101273, 1993.
- 1500 van der Molen, J., Aldridge, J., Coughlan, C., Parker, E., Stephens, D., and Ruardij, P.: Modelling marine ecosystem response to climate change and trawling in the North Sea, *Biogeochemistry*, 113, 213–236, doi:10.1007/s10533-012-9763-7, 2013.
- van Leeuwen, S., Tett, P., Mills, D., and van der Molen, J.: Stratified and non-stratified areas in the North Sea: long-term variability and biological and policy implications, *J. Geophys. Res.-Oceans*, 120, doi:10.1002/2014JC010485, 2015.
- 1505 Vaquer-Sunyer, R., and Duarte, C. M.: Thresholds of hypoxia for marine biodiversity, *P. Natl. Acad. Sci. USA*, 105(40), 15452–15457, doi:10.1073/pnas.0803833105, 2008.
- von Westernhagen, H., Hickel, W., Bauerfeind, E., Niermann, U., and Kröncke, I.: Sources and effects of oxygen deficiencies in the south-eastern North Sea, *Ophelia*, 26, 457–473, doi:10.1080/00785326.1986.10422006, 1986.
- 1510 Wanninkhof, R.: Relationship between wind speed and gas exchange, *J. Geophys. Res.*, 97, 7373–7382, doi:10.1029/92JC00188, 1992.

Weston, K., Fernand, L., Nicholls, J., Marca-Bell, A., Mills, D., Sivy, D., and Trimmer, M.: Sedimentary and water column processes in the Oyster Grounds: a potentially hypoxic region of the North Sea, *Mar. Environ. Res.*, 65, 235–249, doi:10.1016/j.marenvres.2007.11.002, 2008.

Table 1. Average critical quantities (2000–2012) characterising the O₂ dynamics in the four different 4×4-regions (see Fig. 2, yellow boxes). Fluxes are cumulated from 1 April to 30 September and relate to a surface layer of thickness $D_{\text{ref}} = 25$ m.

region		A – SNS	B – SCNS	C – NCNS	D – NNS
PP _{mid}	g C m ⁻²	169.0	147.8	134.6	148.1
ADH _{org,in}	g C m ⁻²	95.9	109.2	92.3	111.0
ADH _{org,out}	g C m ⁻²	89.2	107.6	92.7	114.4
EXP _{org}	g C m ⁻²	23.4	17.5	16.2	18.4
MIX _{O₂}	g O ₂ m ⁻²	116.1	66.7	13.7	18.2
initial O ₂	mg O ₂ L ⁻¹	10.1	9.9	9.5	9.5
final O ₂	mg O ₂ L ⁻¹	7.7	7.9	8.0	8.3
t_{strat}	days	80	151	220	226
D_{mid}	m	11.4	14.7	23.1	25.7
D_{bot}	m	39.6	43.5	93.0	113.4
area	km ²	7643.1	7454.3	7108.9	6677.2
V_{sub}	km ³	111.3	138.0	483.3	590.5

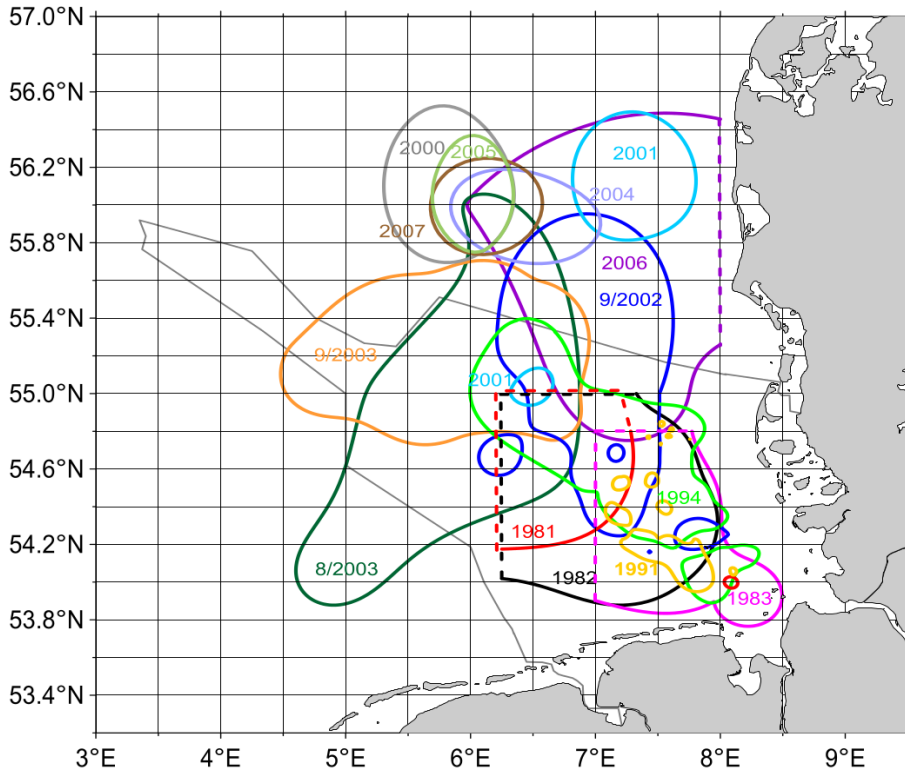


Figure 1. Extent of observed O_2 concentrations $< 6 \text{ mg O}_2 \text{ L}^{-1}$ in the German Bight area from 1980 to 2010. Survey limitations are indicated by dotted lines Dotted lines indicate geographical limits of the individual surveys. Light grey line marks German Maritime Area (from Topcu and Brockmann, 2015).

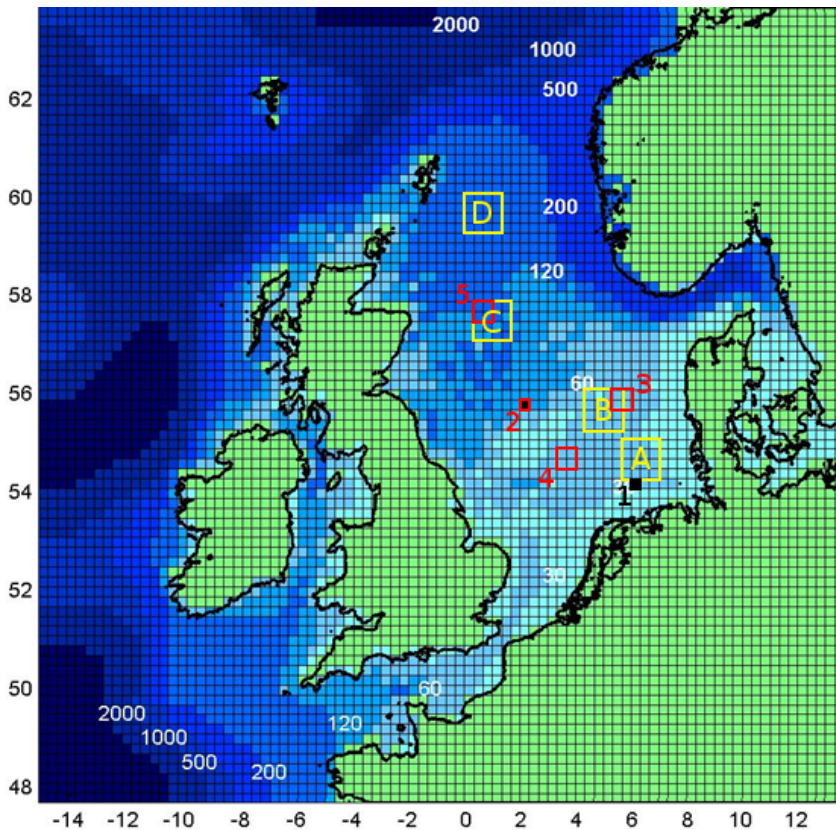


Figure 2. Horizontal grid and bottom topography of the HAMSON-ECOAM model domain. White numbers indicate depth levels. Yellow boxes A–D mark the 4×4 -regions used for the characterisation of key features presented in Sect. 3.3. Black-filled boxes (1, 2) mark the validation sites discussed in Sect. 3.1.1 Red-framed boxes (2–5) indicate regions used for the O_2 mass balance calculations in Sects. 3.4–3.7.

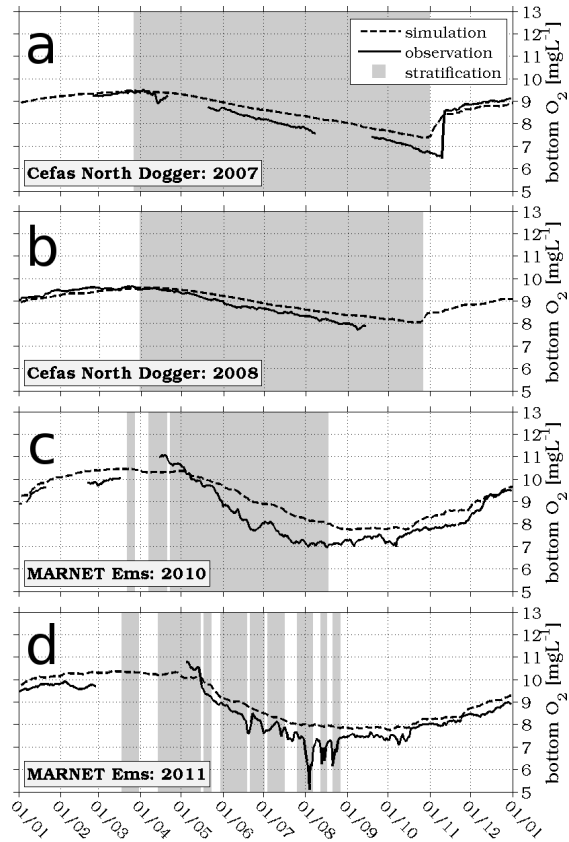


Figure 3. Annual time series of observed and simulated bottom O₂ concentrations at Cefas station North Dogger in (a) 2007 and (b) 2008, and at MARNET station Ems in (c) 2010 and (d) 2011. Same legend for all panels. Grey shaded areas indicate the stratification periods derived from simulated T according to Eq. (1).

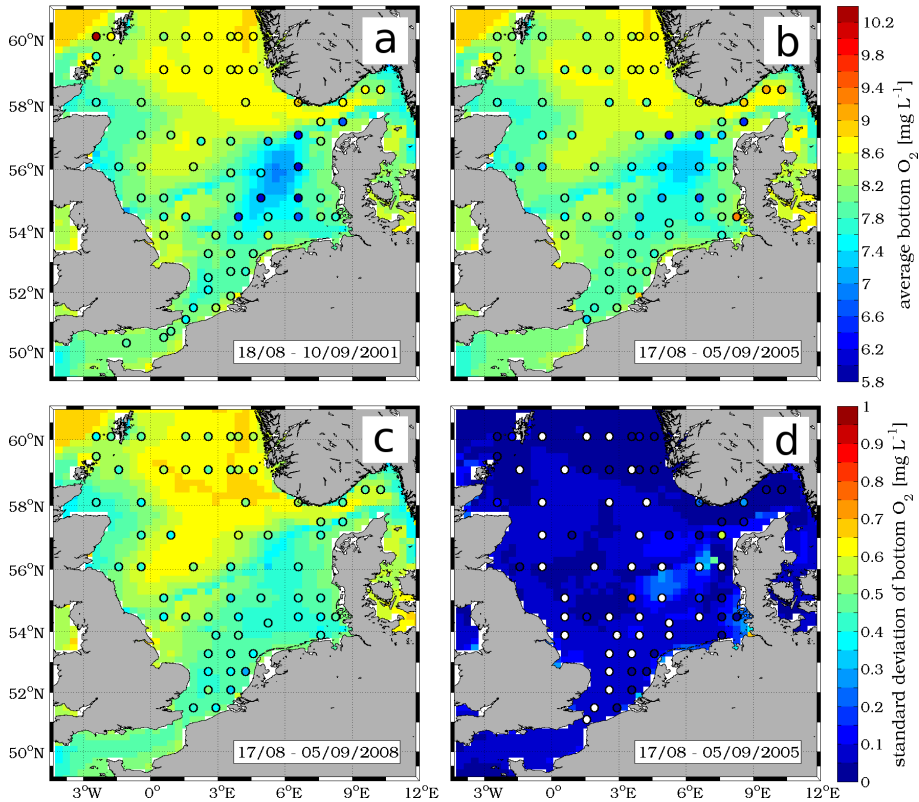


Figure 4. Spatial distribution of observed and simulated average bottom O₂ concentrations in late summer (a) 2001, (b) 2005 and (c) 2008, and (d) standard deviation in 2005. Colour scale of panel (b) applies to panels (a–c). Circles indicate sample sites, underlying colours show simulation results. Averages and standard deviation were calculated for the entire observation period (bottom-left corner of each panel). White circles in (d) mark model bottom grid cells with only one corresponding observed value (i.e., no standard deviation).

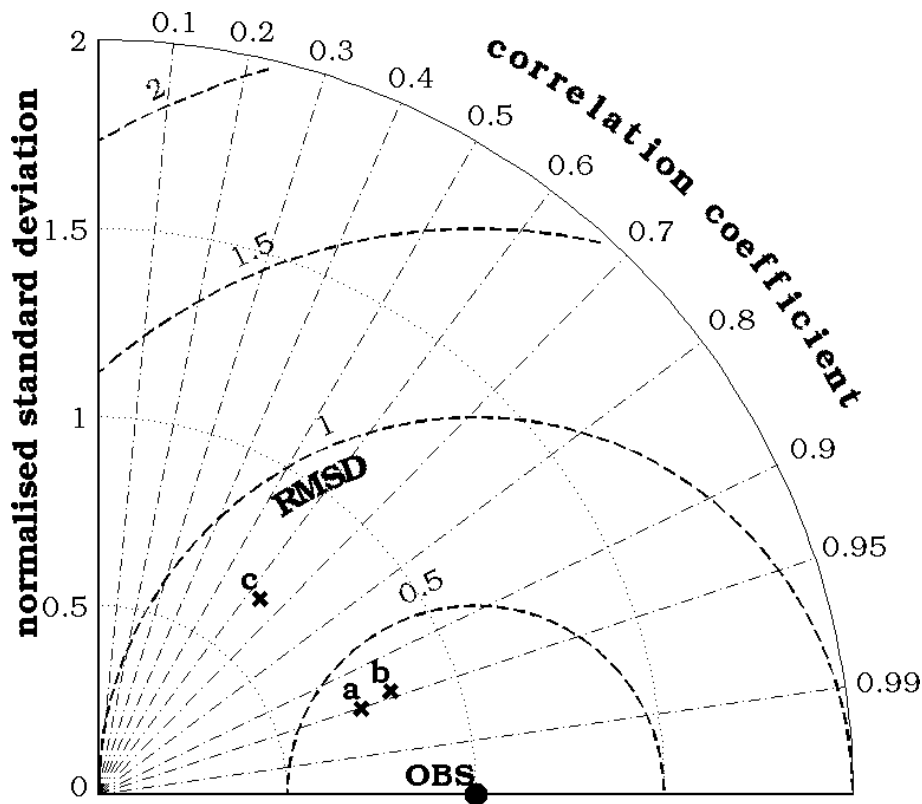


Figure 5. Taylor diagram of simulated (\times) bottom O_2 concentrations compared to observations (OBS) for time series (see Fig. 3) at **(a)** Cefas North Dogger and **(b)** MARNET Ems, and **(c)** spatially resolved data (see Fig. 4). Standard deviations and centred root-mean-square differences (RMSD) were normalised by the standard deviation of the corresponding observations.

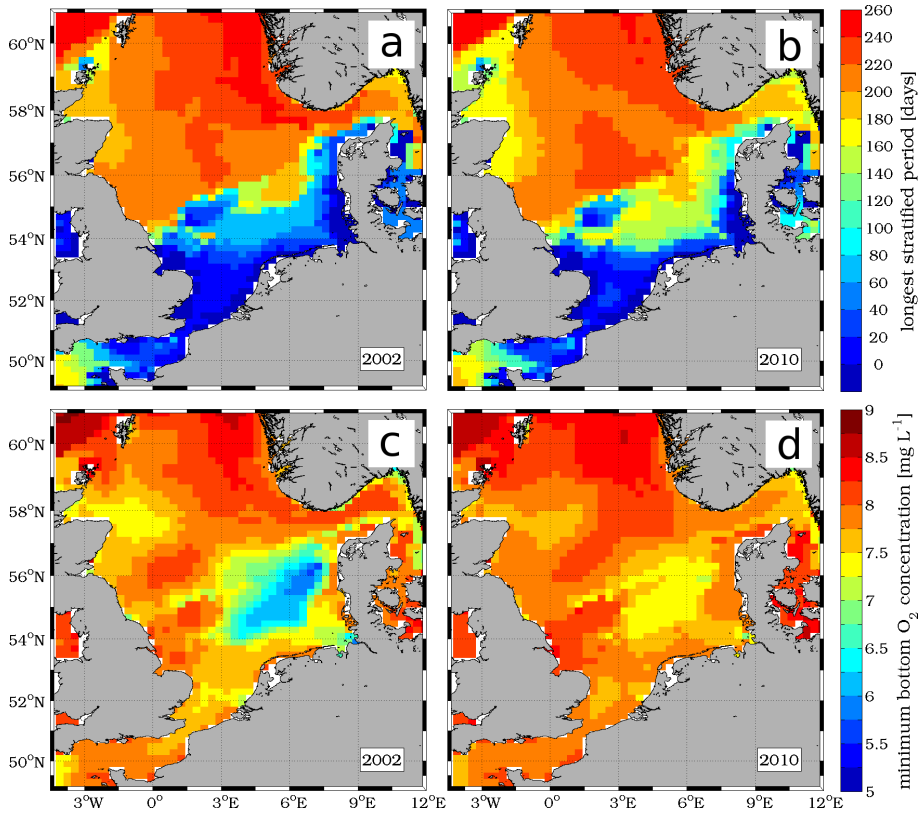


Figure 6. Spatial distributions of (a, b) longest continuous stratification period derived from simulated T according to Eq. (1) and (c, d) simulated annual minimum bottom O₂ concentrations for the years 2002 (a, c) and 2010 (b, d). Same colour scales for (a, b), and (c, d).

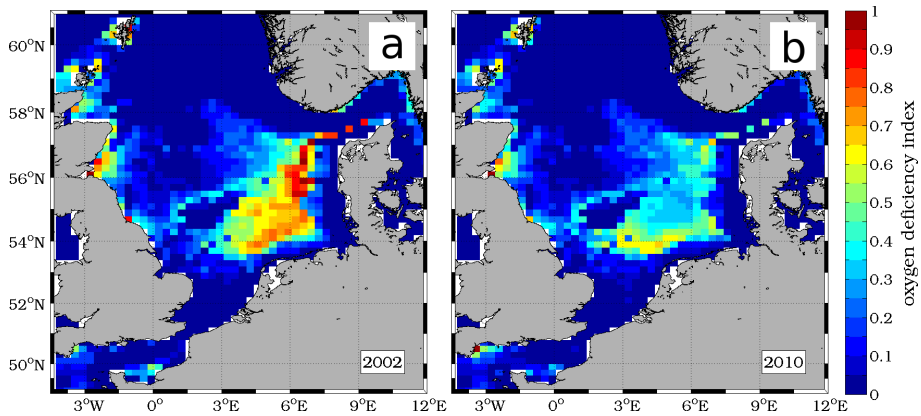


Figure 7. Spatial distribution of oxygen deficiency index (ODI) according to Eq. (5) for the years 2002 (a) and 2010 (b).

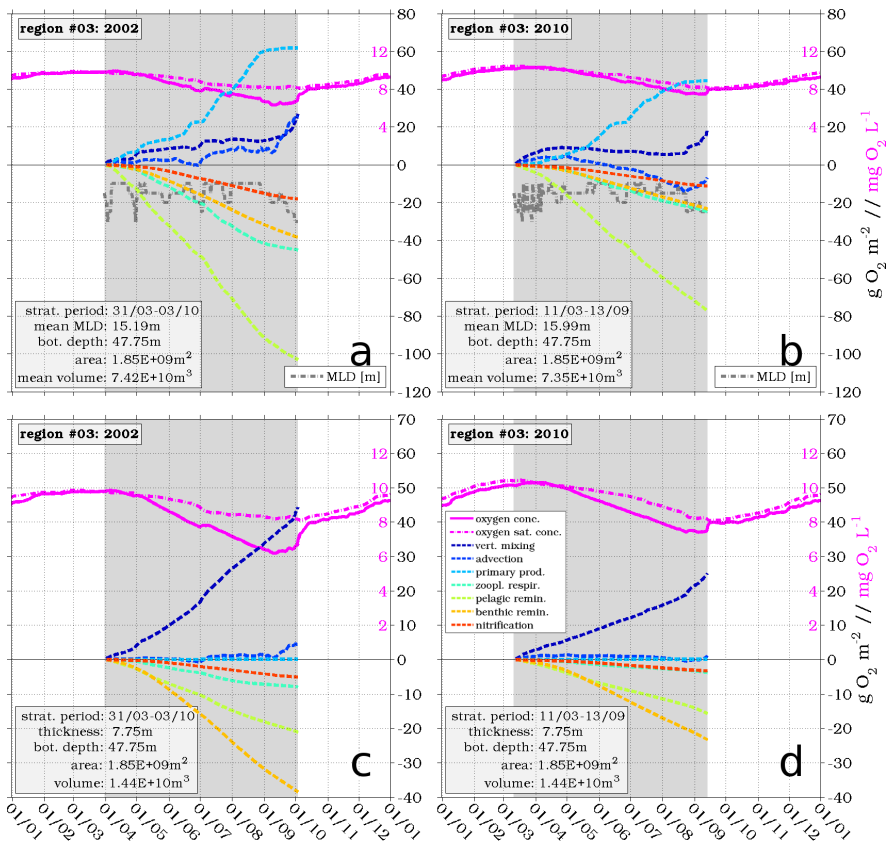


Figure 8. Mass balances of simulated O_2 in region 3 (see Fig. 2) during stratification (grey shaded): **(a, b)** for the entire volume below the MLD (grey dash-dotted; according to Eqs. (1) and (2)), and **(c, d)** only for the bottom layer for the years 2002 **(a, c)** and 2010 **(b, d)**. Same legend for all panels. Black y axes apply to processes, magenta y axes apply to O_2 (saturation) concentrations. Values of black y axes in **(a, b)** also apply to MLD (unit: m). Changes in O_2 due to different processes are cumulative. Text boxes list relevant stratification parameters, average volume of the analysed water body and bottom depth. Note different y axes for **(a, b)** and **(c, d)**.

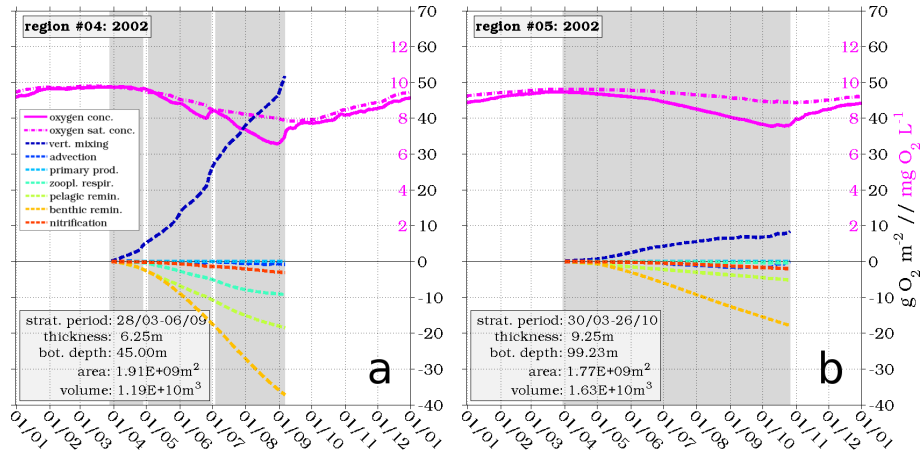


Figure 9. Mass balances of simulated bottom O_2 in regions 4 (a) and 5 (b); (see Fig. 2) during stratification (grey shaded) in 2002. Same legend for (a, b). Black y axes apply to processes, magenta y axes apply to O_2 (saturation) concentrations. Changes in O_2 due to different processes are cumulative.

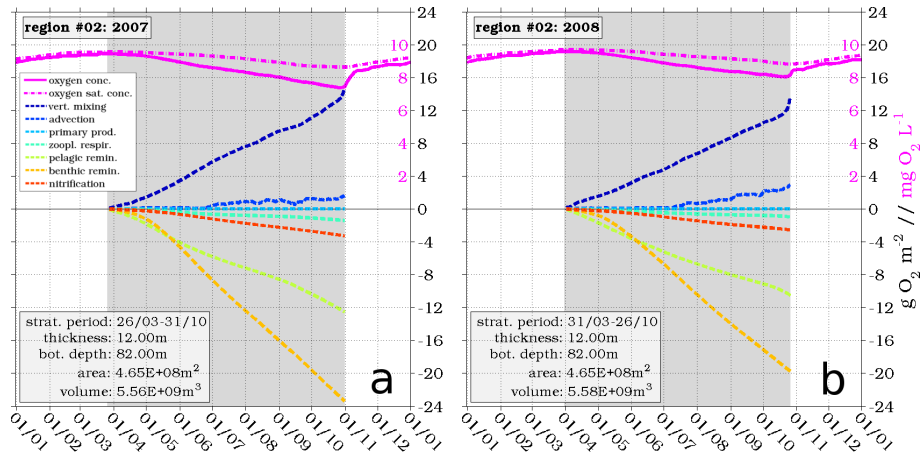


Figure 10. Mass balances for simulated bottom O_2 at Cefas North Dogger (see Fig. 2, region 2) during stratification (grey shaded) in (a) 2007 and (b) 2010. Same legend for (a, b). Black y axes apply to processes, magenta y axes apply to O_2 (saturation) concentrations. Changes in concentrations due to different processes are cumulative.

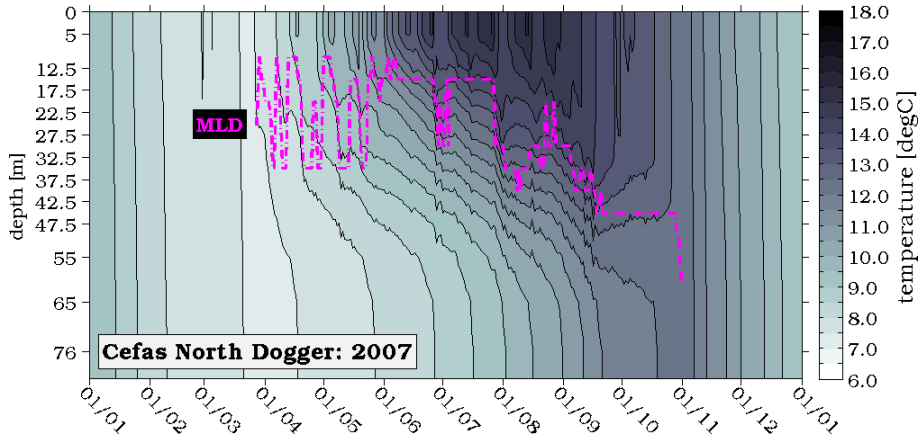


Figure A1. Hovmöller diagram of simulated T and MLD according to Eqs. (1) and (2) at Cefas station North Dogger (see Fig. 2, region 2) in 2007. Depth levels represent the centre depth of model layers.